

GROUND WATER FLOW CONDITIONS RELATED TO THE PRE-BASALT  
BASEMENT GEOMETRY DELINEATED BY GRAVITY MEASUREMENTS  
NEAR KAMIAK BUTTE, EASTERN WASHINGTON

A Thesis

Presented in Partial Fulfillment of the Requirements for the

Degree of Master of Science

With a

Major in Hydrology

In the

College of Graduate Studies

University of Idaho

By

Derek Holom

May 2006

Major Professor: Dr. James L. Osiensky

**AUTHORIZATION TO SUBMIT THESIS**

This thesis of Derek Holom, submitted for the degree of Master of Science with a major in Hydrology and titled “Ground water flow conditions related to the pre-basalt basement geometry delineated by gravity measurements near Kamiak Butte, eastern Washington,” has been reviewed in final form. Permission, as indicated by the signatures and dates given below, is now granted to submit final copies to the College of Graduate Studies for approval.

Major Professor \_\_\_\_\_ Date \_\_\_\_\_  
James L. Osiensky, Ph. D.

Committee  
Members \_\_\_\_\_ Date \_\_\_\_\_  
John S. Oldow, Ph. D.

\_\_\_\_\_ Date \_\_\_\_\_  
Jan Boll, Ph.D.

Department  
Administrator \_\_\_\_\_ Date \_\_\_\_\_  
Dennis J. Geist, Ph.D.

Discipline’s  
College Dean \_\_\_\_\_ Date \_\_\_\_\_  
Judith T. Parrish, Ph.D.

Final approval and acceptance by the College of Graduate Studies

\_\_\_\_\_ Date \_\_\_\_\_  
Margrit von Braun

**Abstract**

Aquifer bottom delineation, to date, in the Palouse ground water basin of eastern Washington and northern Idaho has been dependent on well logs for deep wells that have penetrated crystalline basement rock. However, only three wells have reached the basement rock complex. Detailed gravity measurements improve the determination of basement rock geometry within a sub-basin on the eastern edge of the Columbia River basalts between Kamiak Butte and Angel Butte near Palouse, Washington. Gravity models greatly decrease geologic conjecture about the geometry of the pre-basalt, crystalline bedrock, surface topography that defines the bottom of the ground water basin. Along the eastern perimeter of the Palouse ground water basin, Columbia River basalts fill steep-sided, dendritic drainages scoured into the underlying crystalline bedrock surfaces. Delineation of these complex boundary conditions is crucial for accurate assessment of the volume of water contained in the basin, and accurate prediction (e.g., numerical models) of future water level declines associated with ground water withdrawals from the basin.

**Acknowledgements**

I would like to thank the Palouse Basin Aquifer Committee (PBAC) for funding this research. I would also like to thank Jim Osiensky, John Oldow, Jan Boll, Mike McVay, Mike August, Brock Hill, Jeff West, Chad Opatz, Eron Singleton, John Bush, and Dean Garwood for all their help with this thesis.

## Table of Contents

Abstract.....	iii
Acknowledgements.....	iv
1 Introduction.....	1
1.1 Statement of Problem.....	1
1.2 Purpose and Objectives.....	1
1.3 Extent of Study Area.....	2
2 Background Information.....	4
2.1 Geology.....	4
2.2 Hydrogeology.....	8
3 Gravity.....	11
3.1 Gravity Surveys.....	12
3.2 Equipment.....	13
3.2.1 Gravimeter.....	13
3.2.2 Global Positioning System (GPS).....	13
3.3 Survey Lines.....	14
3.4 Gravity Data Reduction.....	14
3.4.1 Ellipsoid Theoretical Gravity.....	16
3.4.2 Latitude Correction.....	16
3.4.3 Atmospheric Correction.....	17
3.4.4 Height Correction.....	17
3.4.5 Bouguer Spherical Cap.....	17
3.4.6 Terrain Corrections.....	18
3.4.7 Complete Bouguer Anomaly.....	18
3.4.8 Regional Trend Removal.....	19
4 Gravity Models.....	21
4.1 Introduction.....	21
4.2 Model Constraints.....	23
4.3 Basement/Valley Fill Density Contrast Model.....	25
4.4 Gravity Line 1.....	27
4.5 Gravity Line 2.....	29
4.6 Gravity Line 3.....	31
4.7 Gravity Line 4.....	33
4.8 Conclusions from the Gravity Models.....	35
5 Predictive Ground Water Model.....	36
5.1 Introduction.....	36
5.2 Basic Model Conditions.....	37
5.3 Simulated Aquifer Test.....	38
5.3.1 Real Aquifer Data.....	38

5.4	Model Simulation.....	41
5.5	Model Calibration.....	43
5.6	Results and Discussion.....	44
5.6.1	Palouse #1.....	44
5.6.2	Palouse City well #2.....	46
6	Conclusions and Recommendations.....	48
6.1	Gravity model conclusions.....	48
6.2	Ground water model conclusions.....	49
6.3	Recommendations.....	50
7	References.....	52
	Appendix A. Absolute Gravity Base Station COLFAX B.....	55
	Appendix B. Gravity Spreadsheet Paper/Spreadsheet Instructions.....	57
	Appendix C. Kamiak Gap Gravity Data.....	74
	Appendix D. Well Logs.....	77
	Appendix E. Structural contour map of the basement in the Kamiak Gap.....	82
	Appendix F. Contour map of the regional Bouguer anomalies.....	83

## List of Figures

Figure 1. Location of the study area within the general area of the Palouse ground water basin.....	2
Figure 2. Site map of the study area outlined in Figure 1. ....	3
Figure 3. Geologic map of the Palouse Basin, excluding the uppermost Palouse loess (Bush, 1998a, 1998b, 2000; unpublished GIS work by Garwood (Bush and Garwood, 2005)).....	5
Figure 4. Diagrammatic stratigraphic column of the general geologic conditions known and “initially assumed” to exist in the Kamiak Gap based on geologic mapping (Bush and Garwood, 2005), personal observations, and evaluation of drillers well logs.....	7
Figure 5. Residual complete Bouguer anomaly contour map, after the regional trend has been removed.....	21
Figure 6. Example of a gravity profile with two blocks (red-purple and blue).....	22
Figure 7. A mean density contrast model for Line 2 (Figure 9). ....	26
Figure 8. Gravity interpretation of Line 1.....	28
Figure 9. Gravity interpretation of Line 2.....	28
Figure 10. Gravity interpretation of Line 3.....	32
Figure 11. Gravity interpretation of Line 4.....	28
Figure 12. The ground water model domain, showing the grid. ....	38
Figure 13. Map of the area outlined in Figure 12, showing the locations of the two pumping wells and all the observation wells used in the aquifer pump test conducted January 31, 2006 (McVay, 2006).....	39
Figure 14. Plot of the changes in water level for all wells used in the ground water model and the change in barometric pressure during the real aquifer pump test (plotted against the primary y-axis (left axis)). ....	40
Figure 15. Plan view of the ground water model outlined in Figure 12. ....	42
Figure 16. Plot of the results from model calibration. ....	44
Figure 17. Plot of the predicted drawdown versus the observed drawdown in Palouse well #1.....	46

Figure 18. Plot of the predicted drawdown versus observed drawdown in Palouse well #2.  
Negative drawdown is water level rise in the well. .... 47

Figure 19. Scatter plot of the difference of Bouguer anomalies between the gravity  
spreadsheet and the values downloaded from the GeoNet server..... 64

## **1 Introduction**

### ***1.1 Statement of Problem***

The main source of water for the inhabitants living above the Palouse ground water basin is the deep Grande Ronde aquifer system. The Palouse ground water basin consists of an area of approximately 1,500 square kilometers (580 square miles) on the eastern fringe of the Columbia River Plateau (Figure 1) and underlies the cities of Pullman, Palouse, and Colfax, Washington; Moscow, Idaho; and the surrounding rural communities. The subsurface geology of the area between Kamiak Butte and Angel Butte in eastern Washington (Figure 1), hereinafter referred to as the Kamiak Gap, is a critical area of hydrogeologic uncertainty relative to the conditions of ground water flow in that portion of the Palouse ground water basin. Location of potential future aquifer recharge projects might depend on whether hydraulic continuity in the Grande Ronde aquifer system exists through the Kamiak Gap.

### ***1.2 Purpose and Objectives***

The purpose of this study was to delineate the subsurface basement configuration through the Kamiak Gap, and evaluate the potential for ground water connection between Palouse and Moscow based on gravity models of the subsurface geology. The general objectives of the study were to conduct a gravity survey within the Kamiak Gap, and use the data collected to generate a gravity based, geophysical model of the subsurface geology with which to help constrain the potential for ground water to flow through the Kamiak Gap.

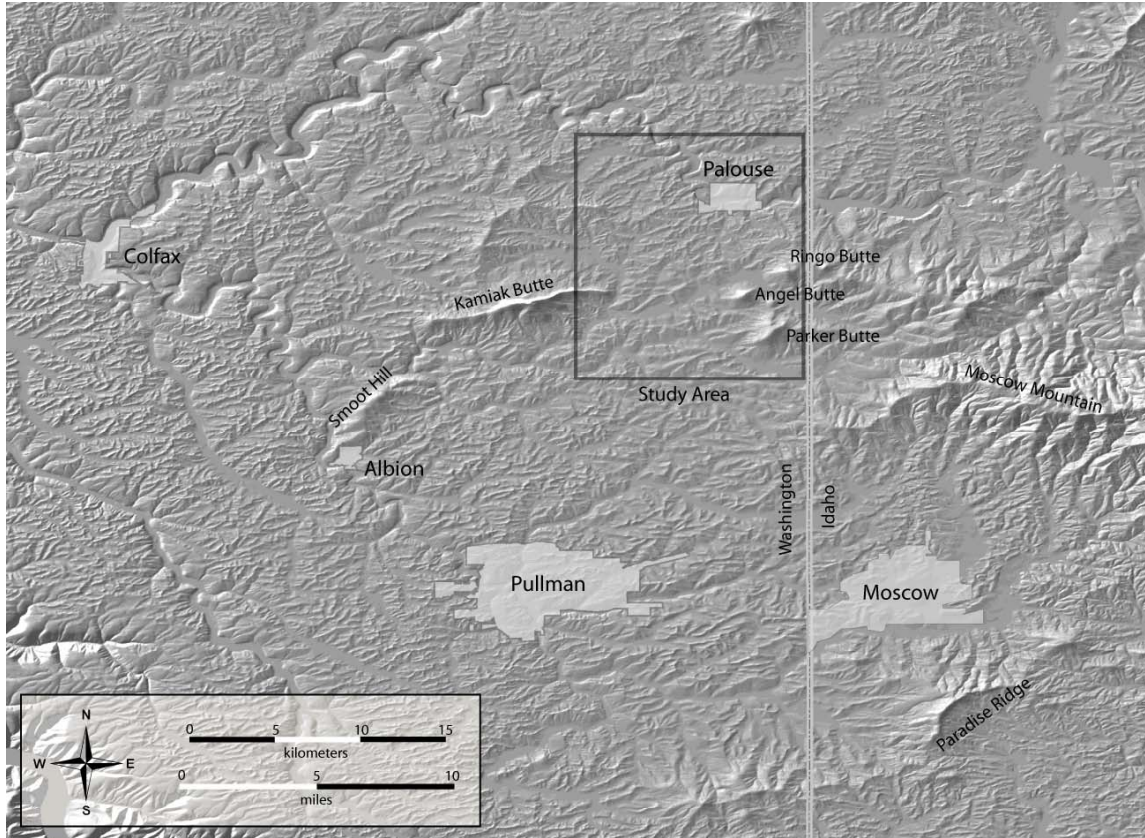


**Figure 1. Location of the study area within the general area of the Palouse ground water basin.**

Specific objectives of this project include:

- 1 Review previous investigations.
- 2 Produce a spreadsheet to calculate gravity anomalies based on current standard methods.
- 3 Generate a gravity model through the Kamiak Gap using GM-SYS™.
- 4 Use existing aquifer data to evaluate potential hydraulic connections through the gap between the city of Palouse, and the cities of Moscow and Pullman.
- 5 Describe potential boundary effects on pumping induced drawdowns based on a hypothetical, numerical ground water model of the Kamiak Gap area.

### ***1.3 Extent of Study Area***

The study area consists of approximately 60 km<sup>2</sup> (24 mi<sup>2</sup>) of mostly private farmland delimited partly by Kamiak Butte to the west and Angel Butte to the east.

Gravity measurements were taken along lines extending north on the railroad tracks past the city of Palouse, and south from the Kamiak Gap along the railroad tracks to Viola Road (Figure 2).

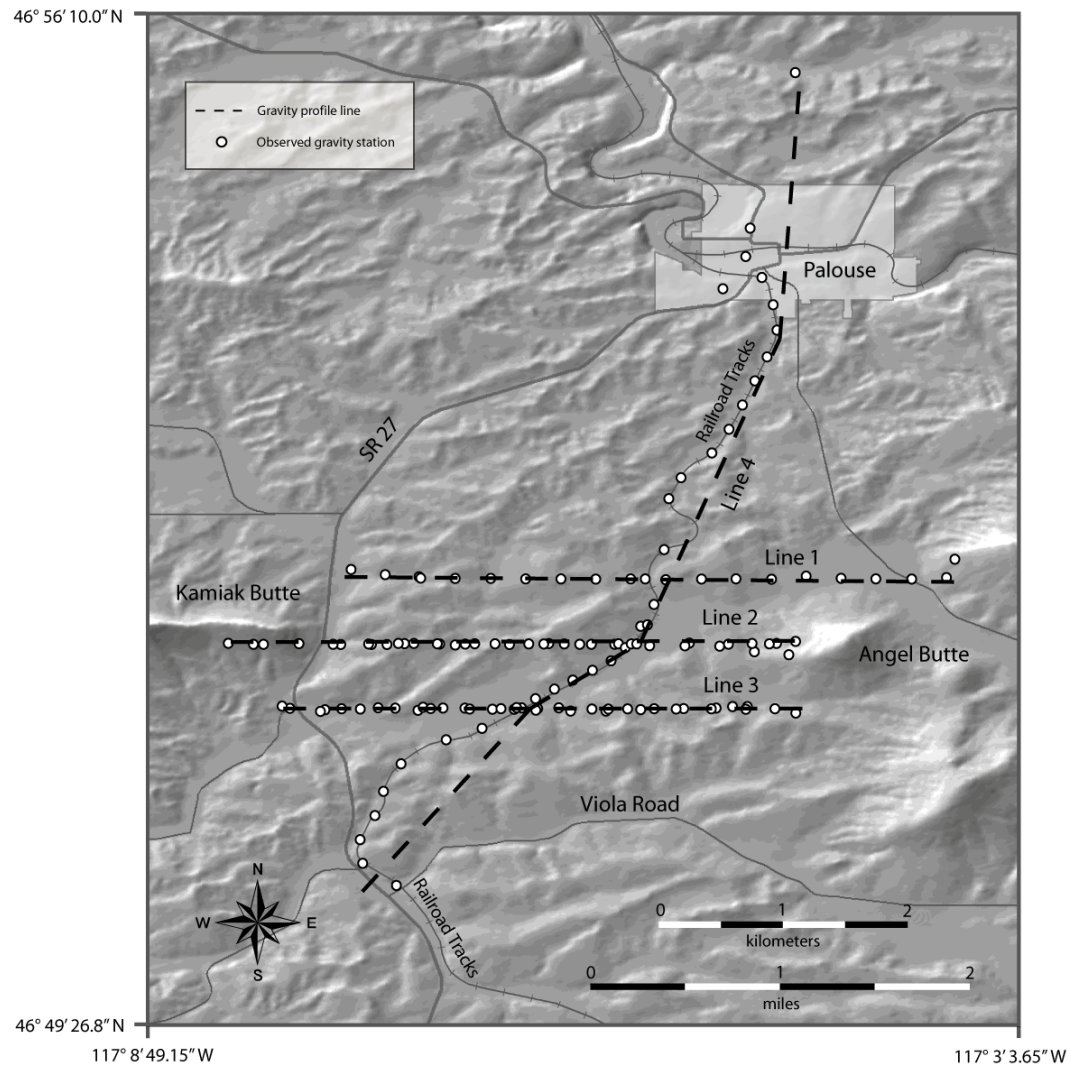


**Figure 2.** Site map of the study area outlined in Figure 1. Gravity survey lines 1, 2, 3, and 4 are shown together with the gravity measurement locations.

## 2 Background Information

### 2.1 Geology

The general geology of the Palouse ground water basin (Figure 3), in ascending stratigraphic order, consists of the pre-basalt basement rocks overlain by the Columbia River Basalt Group (CRBG) and its sedimentary interbeds of the Latah Formation. These units are overlain by Miocene sediments and Pleistocene loess, as well as Holocene alluvium and colluvium (Gullick, 1994).

The pre-basalt crystalline basement complex is composed of metamorphic and igneous rocks. These crystalline rocks are considered to form the eastern boundaries of the ground water basin. These rocks include the undifferentiated Cretaceous granites (Kgr) of Moscow Mountain, Paradise Ridge and Bald Butte; the pre-Cretaceous (€qk) quartzites of Kamiak Butte; the Precambrian gneiss, argillite, siltite and quartzite north of Kamiak Butte (p€gasq); and the Precambrian quartzites, gneiss, and schist (p€qgs) of Angel Butte, Parker Butte, Ringo Butte and Tomer Butte (Duncan, 1998; Gulick, 1994; Provant, 1995).

During the Miocene, from approximately 17 to 6 Ma, flood basalts of the Columbia River Basalt Group were extruded from fissures and vents in northeastern Oregon, emplacing approximately 174,000 km<sup>3</sup> (approximately 42,000 mi<sup>3</sup>) of basalt (Tolan et al., 1989). The CRBG is defined by six major formations. Four formations are present in the Palouse ground water basin; from oldest to youngest the formations include: Imnaha, Grande Ronde, Wanapum and the Saddle Mountains basalts. In the Palouse ground water basin, the Imnaha basalt has only been observed in Washington State University Well #7, which penetrated to a depth of 671 meters (2224 feet) from the

land surface before being backfilled to 546 meters (1814 feet). The Imnaha basalt thins to the east and is not encountered in the Moscow area due to elevational rises in the basement between Moscow and Pullman.

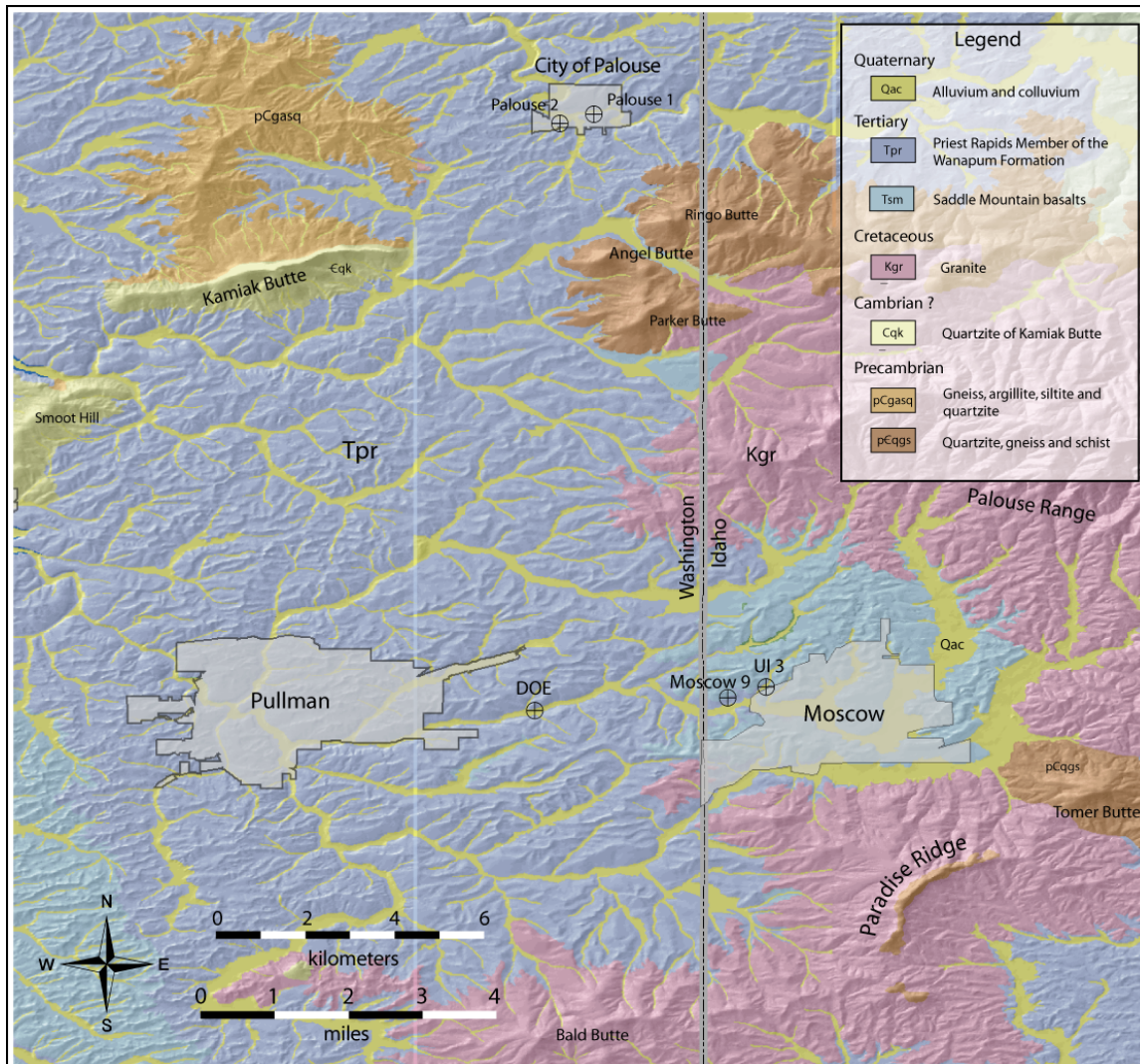


**Figure 3. Geologic map of the Palouse Basin, excluding the uppermost Palouse loess (Bush, 1998a, 1998b, 2000; unpublished GIS work by Garwood (Bush and Garwood, 2005)). The locations for wells Moscow 9, UI 3, DOE, Palouse 2 and Palouse 1 are shown for reference.**

The Grande Ronde Formation is separated into four different units based on magnetic polarity; from oldest to youngest these include the magnetostratigraphic units R1, N1, R2 and N2 (Tolan et al., 1989). The Grande Ronde is the most voluminous basalt formation of the CRBG, comprising approximately 87% of the total volume of

basalt (Tolan et al., 1989). The Grande Ronde is present throughout the Palouse ground water basin; however, differences exist in the extent and volume of emplacement forming the different geologic sub-basins. In the Moscow area, the thickness of the Grande Ronde is over 304 m (1000 ft) in places; however, approximately 60% of the basin fill by volume consists of interbedded sediments of the Latah Formation (Bush, 1998a, 2000, 2005).

In the Pullman area, the Grande Ronde is folded, exhibiting northwest trending anticlines and synclines, and a subsurface monoclinial feature that dips east towards Moscow (Bush, 2005). The thickness and total volume of the Grande Ronde basalt are greater in Pullman than in the Moscow area due to an increased depth to basement, and decreased thickness of interbedded sediments of the Latah Formation (Bush, 1998).

The thickness of the Grande Ronde basalt in Palouse, Washington is not well known, and the lateral continuity of the Grande Ronde formation through the Kamiak Gap has not been established. The subsurface distribution of units established from geologic mapping by Bush and Garwood (2005), my observations, and logs from private wells drilled in the Kamiak Gap (Figure 4) includes, from the top downward, loess of the Palouse Formation, the Priest Rapids Member of the Wanapum Formation, and the sediments of the Latah Formation. No wells encounter Grande Ronde at depth, but the wells are not deep enough to intercept basement. Thus, the continuity of the Grande Ronde through the Kamiak Gap is at question and represents a primary research objective of this project.

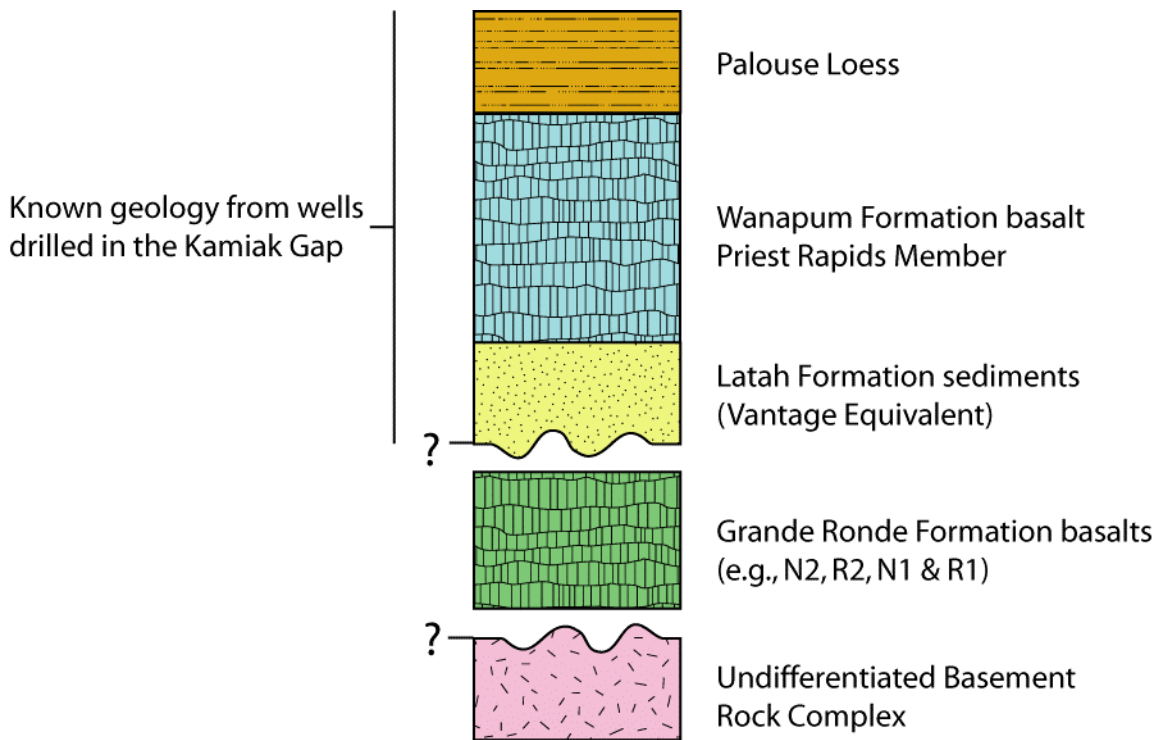


**Figure 4. Diagrammatic stratigraphic column of the general geologic conditions known and “initially assumed” to exist in the Kamiak Gap based on geologic mapping (Bush and Garwood, 2005), personal observations, and evaluation of drillers well logs.**

The Latah Formation consists of spatially variable deposits of gravel, sand and clay underlying, overlying and interbedded within the basalt flows of the CRBG. In Moscow and Palouse, the Latah Formation sediments separate the upper basalt flow of the Grande Ronde Formation from the Priest Rapids Member of the Wanapum Formation; however, in Pullman the Priest Rapids Member is mostly in direct contact with the N2 magnetostratigraphic unit of Grande Ronde Formation except for sparse, interbedded channel deposits of sediments (Bush, 2005). The thickness of the Latah Formation sediments diminishes greatly west of Moscow about 1.6 kilometers (1.0 miles) from the Idaho-Washington border. In Palouse, the Latah Formation sediments are continuous to the south through the Kamiak Gap, but pinch out towards Pullman.

Two members of the Wanapum Formation exist in the Palouse ground water basin; these are the older Roza Member and younger Priest Rapids Member. The Roza basalts are present only in the western portions of the basin; they pinch out against topographically higher basalts (structurally deformed) of the Grande Ronde Formation in the Pullman area, and the pre-basalt crystalline basement highs of Kamiak Butte, Smoot Hill, and subcrops of metamorphic basement rocks to the north near the town of Palouse (Bush and Garwood, 2005) (Figure 3). The Priest Rapids Member, however, is ubiquitous within the Palouse ground water basin, and is laterally continuous through the Kamiak Gap; the average thickness of the Priest Rapids Member is about 61 m (200 ft) (Duncan, 1998).

The Palouse Formation constitutes the characteristic rolling hills overlying the Palouse ground water basin. These hills are made up of the eolian loess deposits of unconsolidated silt and fine sands ranging in thickness from a few centimeters to tens of meters (Gulick, 1994). The loess was deposited directly on top of basalts of Wanapum Formation in most of the Palouse basin, except for the Moscow area, where the loess overlies sediments of Bovill of the Latah Formation (Bush, 1998; Bush, 2000).

## ***2.2 Hydrogeology***

The general hydrogeology of the Palouse ground water basin consists of the deep, confined, Grande Ronde basalt aquifer system, separated from the upper, confined Wanapum basalt aquifer system by a thick sedimentary interbed of the Latah Formation. The interbed is considered to be equivalent chronologically to the Vantage Member of the Ellensburg Formation in central Washington, and locally forms both aquitards and aquifers depending on the grain size distribution. Most municipal wells in the basin are

completed in and draw water from the Grande Ronde aquifer system and associated Latah Formation interbeds. However, the Latah Formation also serves as a local aquifer system for some private wells in the area.

In the Moscow area, the Palouse ground water basin is bounded to the north, east and south by outcrop exposures of crystalline rocks of the Palouse Range, Tomer Butte, Paradise Ridge, Bald Butte, and smaller unnamed hills, creating a horseshoe-shape. In the Pullman area, the ground water basin is bounded to the northwest by crystalline rocks of Smoot Hill, and to the north by crystalline rocks of Kamiak Butte; however, little is known about the potential boundary conditions to the west and southwest. The city of Palouse sits in a bowl-like feature at the land surface, with visible exposures of crystalline rock ridges and buttes in almost all directions except for the gap between Kamiak Butte and Angel Butte, and a gap to the west toward Colfax, Washington.

For the past four decades, ground water monitoring has shown a steady water level decline of about 30 to 45 centimeters (1 to 1.5 feet) per year in the Grande Ronde aquifer system (Owsley, 2003). Artificial recharge projects were proposed in the early 1960's to maintain the supply of ground water in the Palouse ground water basin (Foxworthy and Washburn, 1963). The present concern over the diminishing ground water resources in the Palouse ground water basin has brought artificial recharge back into consideration as a potential remedy for declining water levels.

Previous conceptual models of the hydrogeology of the Palouse ground water basin suggested that the natural discharge from the Grande Ronde aquifer system was to the southwest into the Snake River. However, Hopster (2004) found that the source of visible spring water discharging into the Snake River is derived from the Wanapum

Formation. To date, no natural discharge from the Moscow/Pullman Grande Ronde aquifer system has been delineated.

Current understanding of short-term ground water flow conditions within the Grande Ronde aquifer system is based on large-scale aquifer tests and suggests the systems is compartmentalized into separate aquifers with no short-term hydraulic interconnectivity (Owsley, 2003). Previous aquifer tests between Moscow and Pullman suggested that some type of ground water “barrier” existed between the cities of Moscow and Pullman near the location of the Washington State Department of Ecology (DOE) well (Figure 3). Recent aquifer tests (McVay, 2006) between Moscow and Palouse have failed to yield concrete evidence of a hydraulic connection in the Grande Ronde aquifer system between Palouse city wells and Moscow wells UI #3, UI #4 and Moscow #9. This suggests the existence of a barrier to ground water flow between the two cities, or that the length of the aquifer tests was too short to cause measurable drawdown over the distance of 20 kilometers (12 miles).

### 3 Gravity

Gravity measurements were recorded in the Kamiak Gap to record the variations in the acceleration of gravity. The variations in gravity along with density measurements of the known geology enable depth to bedrock predictions.

Gravity is the force of attraction between two or more bodies. For a smaller body of mass,  $m$ , and a larger body of mass,  $M$ , the attraction is related proportionally by the product of the two masses and inversely proportional to the distance,  $r$ , between the bodies (Lowrie, 2004) as:

$$F = \frac{-GmM}{r^2} \quad (1)$$

where:

$F$  is the force of gravity in units of  $N$ ,

$G$  is the universal gravitational constant, empirically calculated to be  $6.6725985 \times 10^{-11} \text{ m}^3\text{kg}^{-1}\text{s}^{-2}$ .

Differences in the density distribution of materials within the Earth produces variations in the gravitational field, which are measured as changes in the gravitational acceleration on the milliGal (mGal) scale. A Gal is named in honor of Galileo Galilee and is an acceleration unit of  $1.0 \text{ cm/s}^2$ ; therefore a milliGal is 1/1000th of a Gal. The total range of gravity on the earth is from 978 Gals at the equator to 983 Gals at the poles. The rotation of the earth about its axis produces centripetal (downward) forces at the poles and centrifugal (outward) forces at the equator. The outward force at the equator is causes what is called the equatorial bulge. This outward force produces a negative effect on the force gravity, thereby decreasing the acceleration of gravity at the equator and

increasing it at the poles. The difference in the acceleration between the equator and the poles is about 5000 mGals (Lowrie, 2004).

### **3.1 Gravity Surveys**

High-resolution measurements of variations in the gravitational force are used to model subsurface variations in density and constitute a useful and cost effective geophysical tool that can aid in the interpretation of the subsurface geology. The usefulness of a gravity survey is contingent on a significant density contrast between valley fill and the host rock; otherwise the contact between valley fill and host rock (bedrock) cannot be distinguished.

An ideal gravity survey consists of a grid pattern of intersecting survey lines with gravity measurements at stations of equal spacing tied into a bedrock control point for each line. Gravity measurements at bedrock control points are important reference points for constraining the geology in gravity models by tying into the host rock. It also provides a point of control for removing regional trends (discussed in § 3.4.8). Every gravity measurement (observed gravity) needs to be corrected to accommodate associated instrument drift and tidal effects. The difference in corrected, observed gravity and the theoretically, predicted gravity at the same location is called a gravity anomaly.

A gravity survey for this investigation consisted of four survey lines. Three of the four lines were oriented east-west with Observed gravity values were compared to the estimated theoretical gravity values for the specific rock types believed to exist along each line. Existing information on the thicknesses and density contrasts for the different geologic units present in the Kamiak Gap was used in the gravity interpretations.

### 3.2 *Equipment*

The equipment used in the gravity surveys included a LaCoste-Romberg gravimeter, and two Leica™ dual-frequency, 500 series GPS receivers with one of the GPS receivers mounted on an all-terrain vehicle (ATV).

#### 3.2.1 *Gravimeter*

The Lacoste-Romberg Model-G Land™ gravity meter has an accuracy of +/- 0.01 mGals. The gravimeter measures the change in the acceleration of gravity when the glass spring expands or contracts when induced by a variation in the force of gravity. To reduce the amount of instrument drift by thermally induced variations in the spring constant, the glass spring is harbored in a sealed, vacuum chamber and is held a constant temperature at all times by an internal heater.

#### 3.2.2 *Global Positioning System (GPS)*

Two Leica 500™ series high-precision GPS receivers were used to delineate the positions of each gravity station. One of the receivers was set up at a nearby National Geodetic Survey marker (U-487) as a base station to reference all of the post-processed points to the World Geodetic System (WGS) 84 ellipsoid; the WGS84 datum agrees with the International Terrestrial Reference Frame (ITRF) to within 10.0 cm (Hinze, 2003). Having a GPS base station continuously record its position for the duration of each survey allows the navigated positions to be corrected for inherent errors associated with time delays or signal refractions. The accuracy of the vertical location for each gravity station is +/- 2.0 cm, which equates to a potential gravity error of +/- 6.0  $\mu$ Gals (0.006

mGals) (Oldow, personal communication, 2006). This amount of error is smaller than the accuracy of the gravimeter.

### **3.3 Survey Lines**

Most of the land in the survey area near the Kamiak Gap is privately owned and farmed, limiting property access to four weeks a year. To minimize the number of individual property owners from which access permission would be required, two roads that run east-west in the Kamiak Gap were chosen as survey lines; these include most of Line 1 and half of Line 3. Line 2 is located entirely on privately owned farmland. The north-south line (Line 4) follows along the railroad tracks from the town of Palouse, Washington to south of the Kamiak Gap near the intersection with Viola Road (Figure 2). Gravity measurements were made at 150-meter (approximately 500 ft) spacings along Lines 1, 2 and 3, and at 300-meter (approximately 1000 ft) spacings along Line 4. Lines 1 and 2 were tied in to a bedrock outcrop for points of control with measurements taken on the eastern flank of Kamiak Butte, and on the western flanks of Angel Butte and Ringo Butte. Line 3 was tied in to two privately owned wells in the Kamiak Gap for points of control and Line 4 was tied in to Palouse City well #2 on the north end of the survey line and tied in to a privately owned well near Viola Road on the south end of the line. Gravity measurements taken near wells for which drillers logs are available help to constrain the gravity models to known subsurface geology.

### **3.4 Gravity Data Reduction**

The procedure for reducing raw gravity includes:

1. Collecting gravity data

2. Post-processing GPS data
3. Entering raw gravity data into a reduction spreadsheet
4. Calculating the terrain corrections separately from the spreadsheet
5. Referencing all collected gravity data to an absolute gravity base station
6. Removing the regional trend using a contouring program that can calculate 1<sup>st</sup>-order, 2<sup>nd</sup>-order and 3<sup>rd</sup>-order polynomials

Specifically, raw gravity data must be corrected for tidal effects, instrument drift, latitudinal variation, height above the 1980 Geodetic Reference System (GRS80) ellipsoid, the mass of the atmosphere, and the mass of the material between the station and the GRS80 ellipsoid (known as the Bouguer spherical cap correction, which is explained in section 3.4.5). The GRS80 ellipsoid was adopted by the International Union of Geodesy and Geophysics (IUGG) as the reference system for gravity calculations. The difference between the ITRF(WGS84) ellipsoid and the GRS80 ellipsoid for gravity reduction is negligible at about 5  $\mu$ Gals (Hinze, 2003). The corrected, observed gravity values are referenced to an absolute gravity base station, and then subtracted from the predicted theoretical gravity at that station to calculate a gravity anomaly (Hinze, 2003). Gravity measurements in the Kamiak Gap are referenced to the International Gravity Standardization Net 1971 station COLFAX B, located in front of the Whitman County courthouse in Colfax, Washington (Appendix A).

A gravity reduction spreadsheet was developed as part of this investigation to calculate gravity anomalies based on the latest standards set by the North American Gravity Database Committee (Hinze, 2003). The paper included in Appendix B describes the methods and calculations used in the spreadsheet, and has been submitted

for review for publication on the Geological Society of America's (GSA) online journal *Geosphere*.

#### 3.4.1 Ellipsoid Theoretical Gravity

The ellipsoid theoretical gravity calculation uses the Somigliana (1930) closed-form formula (equation 2) based on the GRS80 ellipsoid to predict the gravity at any latitude  $\varphi$  north or south (Hinze, 2003).

$$g_{\varphi} = g_e \frac{1 + k \sin^2 \varphi}{\sqrt{1 - e^2 \sin^2 \varphi}} \quad (2)$$

where values for the GRS80 reference ellipsoid are:

$g_{\varphi}$  is the ellipsoid theoretical gravity,

$g_e = 978032.67715$  mGals, and is the acceleration of gravity at the equator,

$k = 0.001931851353$  is a dimensionless coefficient, and

$e^2 = 0.0066938002290$  is a dimensionless coefficient.

#### 3.4.2 Latitude Correction

The latitude correction accounts for the change in gravity with respect to the location of the poles of the Earth. Latitude corrections are referenced to the latitude of the absolute gravity base station COLFAX B. The following formula is used to calculate the change in gravity per kilometer (Lowrie, 2004):

$$g_L = 0.8108 \sin(2\varphi)d \quad (3)$$

where:  $g_L$  is the latitude correction (mGals),

$d$  is distance of the gravity station from the absolute gravity base station (km), and

$\varphi$  is the latitude of the gravity station.

### 3.4.3 Atmospheric Correction

The mass of the atmosphere is unaccounted for in the theoretical gravity calculation and must be subtracted from the observed gravity. The atmospheric correction uses the height  $h$  of the gravity station in meters above the GRS80 ellipsoid in the following equation (Hinze, 2003):

$$g_{atm} = 0.874 - 9.9 \times 10^{-5} h + 3.56 \times 10^{-9} h^2 \quad (4)$$

where :  $g_{atm}$  is the atmospheric correction (mGals).

### 3.4.4 Height Correction

The magnitude of observed gravity decreases with increasing distance from the center of the Earth. In order to be compared with the theoretical gravity at the same location, the height of the gravity station must be corrected to the WGS84 ellipsoid as follows (Hildebrand, 2003; Hinze, 2003):

$$g_h = -(0.3087691 - 0.0004398 \sin^2 \varphi)h + 7.2125 \times 10^{-8} h^2 \quad (5)$$

where:

$g_h$  is the height correction (mGals),

$h$  = the height of the gravity station in meters above the WGS84 ellipsoid, and

$\varphi$  = the latitude of the gravity station.

### 3.4.5 Bouguer Spherical Cap

The Bouguer spherical cap correction sets the observed gravity value to a standard density based on either the average density of the continental crust ( $2.67 \text{ g/cm}^3$ ) or to a site-specific average density of the basement rock for local surveys. Older methods of

reducing gravity data used a similar correction called the Bouguer slab, which was based on a flat Earth model. The Bouguer spherical cap correction is the new standard formula that accounts for the curvature of the Earth (Hinze, 2003):

$$g_{SC} = 2\pi G\rho(\mu h - \lambda R) \quad (6)$$

where:  $\mu$  and  $\lambda$  are dimensionless coefficients (LaFehr, 1991),

$g_{SC}$  is the spherical cap correction (mGals),

$G$  = Newton's gravitational constant =  $6.6725985 \times 10^{-11} \text{ m}^3/\text{kg}\cdot\text{s}^2$ ,

$\rho$  = density of the spherical cap, usually  $2670 \text{ kg/m}^3$ ,

$h$  is height of the gravity station above the GRS80 reference ellipsoid (km), and

$R$  is the height of the gravity station above the WGS84 ellipsoid plus the average radius of the Earth (km).

#### 3.4.6 *Terrain Corrections*

To account for the effects of topography in the survey area the terrain corrections calculate the mass excesses and mass deficits of the topography near a gravity station. The terrain corrections used in this survey were calculated using InnerTC and OuterTC, software packages that access digital-terrain data sets based on the methods developed by Donald Plouff (Cogbill, 1990). The observed gravity was corrected for terrain effects out to 166.7 km (104.2 mi).

#### 3.4.7 *Complete Bouguer Anomaly*

The complete Bouguer anomaly is the difference between the corrected, observed gravity and the theoretical gravity. An anomalously high gravity value indicates the presence of a geologic body of higher density than the basement rock; whereas an

anomalously low gravity value indicates a geologic body of lower density. The complete Bouguer anomaly ( $g_{BA}$ ) is calculated as follows:

$$g_{BA} = g_m - g_\phi + g_L + g_h - g_{am} + g_{SC} - g_T \quad (7)$$

where:  $g_m$  is the tide and drift corrected, measured gravity, and  $g_T$  is the terrain correction, and all other terms are as described previously.

#### 3.4.8 Regional Trend Removal

Measurements of the observed gravity in small scale, local surveys, such as the survey conducted in the Kamiak Gap, are often masked by much larger, regional gravity signals. These regional gravity signals are produced by large geologic bodies, such as a low-density root zone of a mountain range (e.g., Rocky Mountains) or a high-density plateau of a basalt embayment (e.g., CRBG). Removal of the regional trend from a local-scale gravity data set, yields residual, complete Bouguer anomalies that are used to model gravity. The regional gravity field in the Palouse ground water basin trends approximately 25° east of north with a gradient of -0.4 mGal per kilometer (Appendix F).

As shown in Figure 5, areas of outcrop exposure at Kamiak Butte and Angel Butte have relatively high gravity anomalies, with anomaly values close to zero mGals. A Bouguer anomaly of approximately zero indicates the average density of the basement rock complex is close to that of the average crustal density of 2.67 g/cm<sup>3</sup>. For this particular survey, negative Bouguer anomalies relative to the basement outcrop Bouguer anomalies infer the presence of less dense geologic material than the quartzite of Kamiak Butte and Angel Butte.

The known geology in the Kamiak Gap consists of low density loess, high density basalt, and low density sediments, all overlying basement of neutral density (i.e., 2.67

g/cm<sup>3</sup>). If, for example, the Kamiak Gap was made up entirely of basalt with an average density of 2.9 g/cm<sup>3</sup> overlying the basement, then the Bouguer anomaly map would show positive Bouguer anomalies between the outcrops of basement rocks on Kamiak Butte and Angel Butte.

The contoured Bouguer anomalies in Figure 5 show the areas of high density and low density materials in the study area. Initial interpretation of the subsurface geology from this map suggests that the warm colored region extending west from Ringo Butte and Angel Butte is an area of shallow depth to basement.

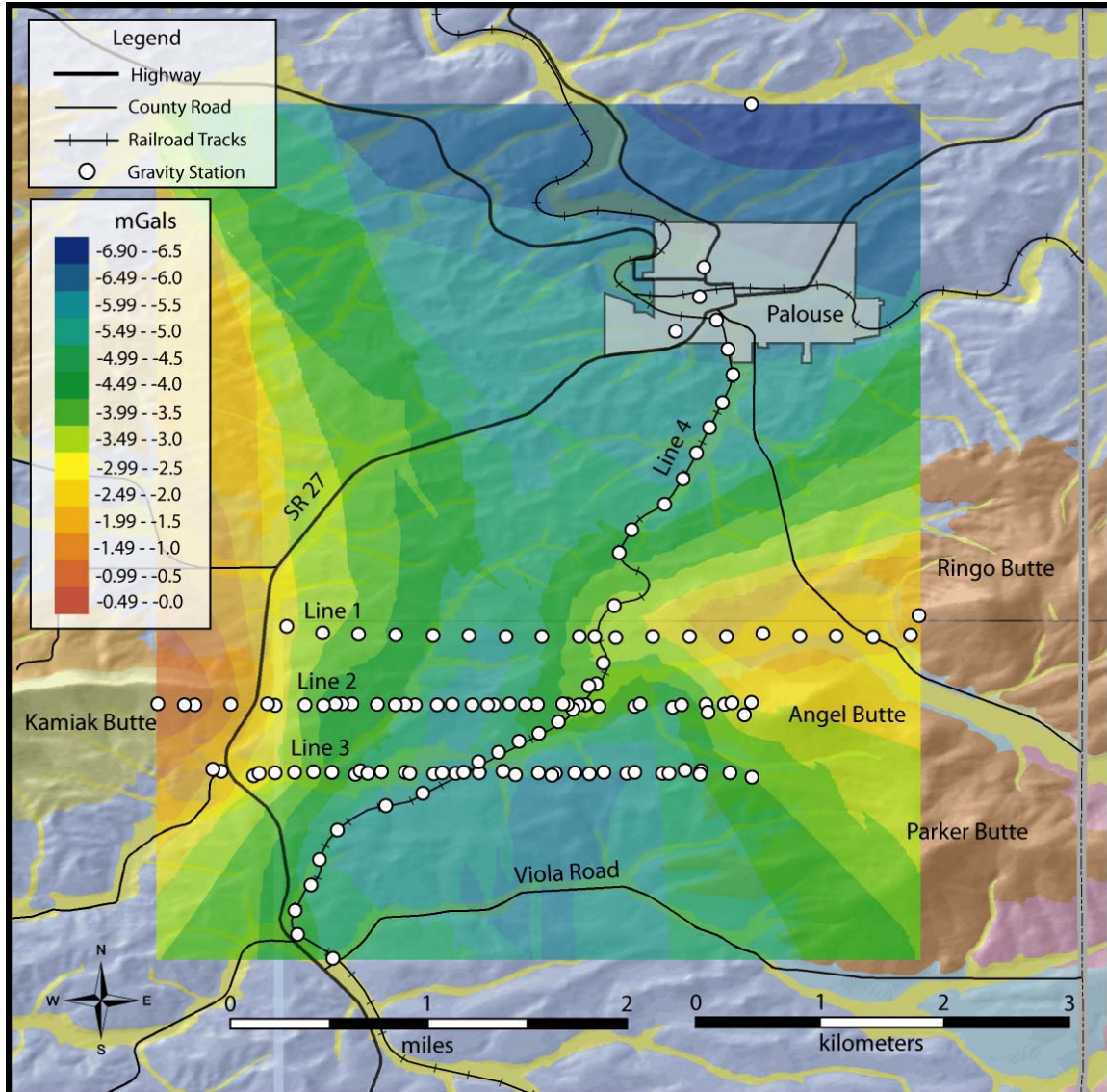


**Figure 5. Residual complete Bouguer anomaly contour map, after the regional trend has been removed. The warm colors represent high gravity anomalies in comparison to the areas of cooler colors.**

## 4 Gravity Models

### 4.1 Introduction

GM-SYST™ is a gravity modeling software program with a graphical, user-interface. It was developed by the Northwest Geophysical Associates, and uses an algorithm based on methods developed by Talwani (1960) for testing the gravity response of a geologic body of arbitrary shape. The gravity data collected during this investigation

are modeled with GM-SYS™ in 2½-dimensions by truncating the length of each block normal to the strike of the profile. Each block is assigned a density value by the user, and the size and shape of each block can be modified graphically in order to match the modeled gravity to the observed gravity. The modeled gravity signal is represented by a black line that changes in response to the change in the shape of a block. Figure 10 is an example that shows how the modeled gravity changes when the size of a block is reduced from its original size in order to match observed gravity points.

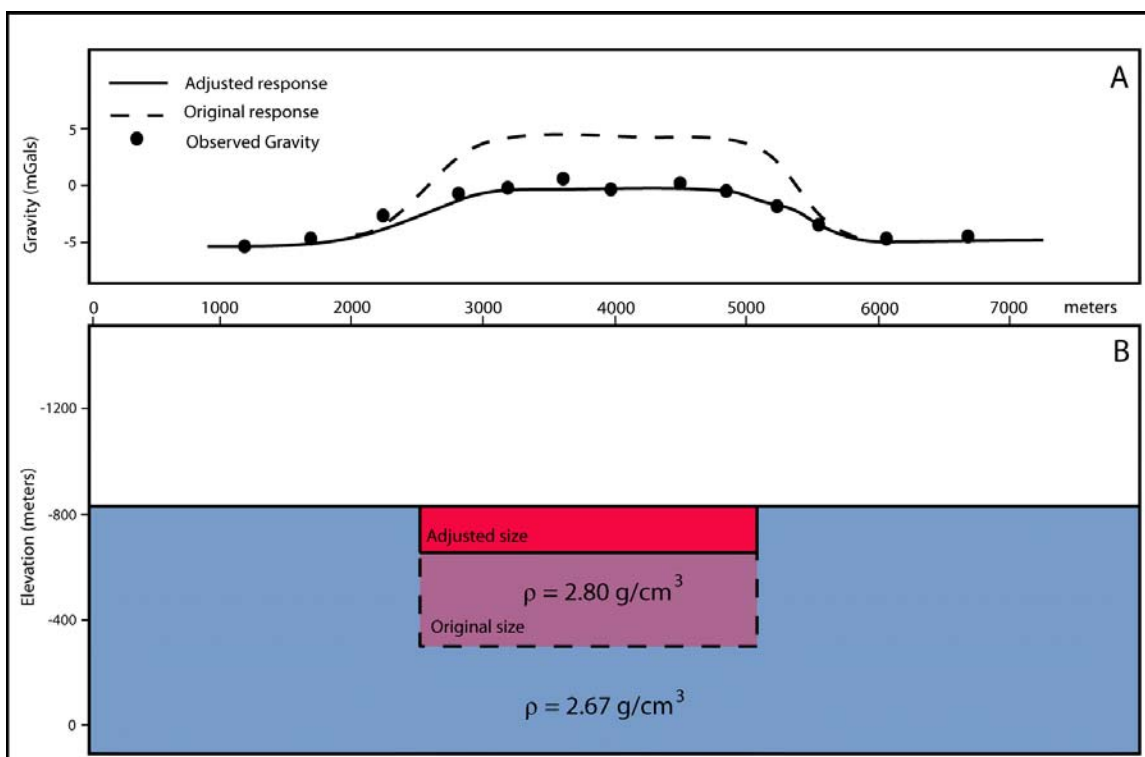


**Figure 6.** Example of a gravity profile with two blocks (red-purple and blue). The red-purple region is the original size of the red block with a density of  $2.80 \text{ g/cm}^3$  inside a larger slab with density of  $2.67 \text{ g/cm}^3$ . The black dots are arbitrary observed gravity points for sake of this example. The dashed black line in window A is the modeled gravity response to the size and shape of the dashed perimeter of the purple block in window B. The solid black line in window A is the gravity response to the adjusted size of the red block, shown with a solid black line perimeter in window B.

#### 4.2 *Model Constraints*

Interpretations of gravity anomalies are non-unique, because any given set of observed gravity anomalies can be modeled to fit an infinite combination of densities and shapes. Bedrock measurements are important control points for gravity models because it ties the other gravity points to an area of solid rock with an assumed constant density.

Gravity measurements near wells that have a record of the lithology (well logs) are also useful in constraining the geology of a gravity model, because they decrease the amount of interpretation. Well logs provided the depth to contacts of different geologic units from the land surface and depending on the depth of the well, it may provide a point of control to bedrock.

In the Kamiak Gap, bedrock gravity measurements were taken at outcrops of pre-Cambrian quartzites. Line 2 starts and finishes at bedrock exposures from the eastern flank of Kamiak Butte to the western slope of Angel Butte. The eastern-most gravity station on Line 1 is the only other bedrock measurement in the study area taken on the western slope of Ringo Butte. To constrain Line 3 and Line 4, the bedrock points were interpreted by overlaying the residual complete Bouguer anomaly contour map (Figure 5) on the geologic bedrock map of the study area (Figure 3). This allows for faux-bedrock measurements to be extrapolated from the overlay, as an alternative to an actual bedrock measurement because the removal of the regional gradient results in a residual gravity anomaly of zero mGals for bedrock outcrops. A gravity anomaly of zero equates to a density of  $2.67 \text{ g/cm}^3$ , which is used for the basement. This procedure results in an uncertainty of +/- 0.5 mGals.

Well logs provided on the Washington Department of Ecology website (WDOE, 2006) were used to interpret the geology as recorded by well drillers. Although none of the wells penetrate basement, gravity measurements taken near all the wells with logs aided in the geologic interpretation of the gravity anomalies.

The densities of quartzite from Kamiak Butte, and basalt from an exposure of the Priest Rapids Member near the gravity base station were determined in the laboratory using a scale and graduated cylinder. Density of Grande Ronde basalt was estimated in the laboratory from core samples of Grande Ronde basalt from the Kendrick, Idaho area (Osiensky, personal communication, 2006).

Profiles of the gravity lines were developed from information found on original driller well logs; however, the profiles incorporate variable estimated densities for the basalt units to account for lithologic variability reported by well drillers. Laboratory measurements of the Grande Ronde basalt core from the Kendrick area resulted in an average density non-vesicular density of  $2.80 \text{ g/cm}^3$  and an average vesicular density of  $2.38 \text{ g/cm}^3$ . The lowest density measurement from the Grande Ronde core was  $2.30 \text{ g/cm}^3$ . The density used for the Grande Ronde basalt in the models was  $2.4 \text{ g/cm}^3$ , based on the vesicular basalt density measurements in the lab and that the Grande Ronde basalt was described mostly as “fractured or broken with water” in Palouse City well #2 well log (Appendix D). Furthermore, a study conducted by the U.S. Geological Survey near Fallon, Nevada found the bulk density of a basalt aquifer to be  $2.25 \text{ g/cm}^3$  with a porosity of 0.16, which would result in an overall density of  $2.41 \text{ g/cm}^3$  when the pore spaces are filled with water (i.e.,  $1.0 \text{ g/cm}^3$ ) (Welch, 2005).

In the Kamiak Gap, strata of Wanapum basalt is reported as “medium basalt” from well driller’s logs and were assigned a density  $2.6 \text{ g/cm}^3$  (average of 2.8 and 2.4) in the models.

**Table 1.** Average density values for geologic units present in study area.

Unit	Samples	Ave. Density ( $\text{g/cm}^3$ )	St. Dev.	Modeled density ( $\text{g/cm}^3$ )
Basement rocks (pKqz)	19	2.62	0.08	$2.67^1$
Grande Ronde (vesicular)	3	2.38	0.07	-
Grande Ronde (non-ves.)	6	2.80	0.12	2.40
Wanapum ( $Mv_{wpr}$ )	20	2.82	0.10	$2.60^2$
Latah sediments (Mc)	-	-	-	$2.00^3$
Palouse loess (Ql)	-	-	-	$1.25^4$

<sup>1</sup>The average density used in the model is  $2.67 \text{ g/cm}^3$  because the anomalies are relative to the average crustal density (i.e.,  $2.67 \text{ g/cm}^3$ ).

<sup>2</sup>Assumed constant density of “medium basalt” as described in well logs.

<sup>3</sup>There are no outcrop exposures of this unit in the area study. The density value used in the gravity models is based on the average density for a sand unit reported in Applied Geophysics (Telford, et al, 1990).

<sup>4</sup>The average density of the Palouse loess is reported in a study conducted in the Palouse region, eastern Washington (King, et al., 2000).

### 4.3 Basement/Valley Fill Density Contrast Model

A simple, two-layer, gravity model presented in Figure 7 was constructed to evaluate the overall density contrast between the valley fill and the basement rock. The result of the best-fit model was a mean density contrast between basement and fill of  $-0.6 \text{ g/cm}^3$  based on a mean valley-fill density of  $2.07 \text{ g/cm}^3$ . The known geology in the Kamiak Gap consists of the Palouse Formation loess, Priest Rapids Member basalt of the Wanapum Formation, sediments of the Latah Formation, and pre-basalt crystalline basement rocks mostly made up of quartzite. In some places, the thickness of the Priest Rapids basalt, as reported in well logs, is greater than 45 meters (150 feet), overlying an indeterminate thickness of Latah Formation sediments. Thickness of Latah Formation sediments is uncertain because all of the wells drilled in the area are completed within the upper 10 meters (33 feet) of sediments, and none of the wells penetrate the entire sequence. The negative density contrast in the Kamiak Gap suggests the presence of a

thick layer of Palouse Loess and Latah Formation sediments, or basalt with a density lower than the average density of the Priest Rapids basalt, such as the pre-CRBG basalt of the Onaway flow. The average density of 15 samples of the Onaway basalt collected near Potlatch, Idaho was determined to be  $2.56 \text{ g/cm}^3$  with a range of  $2.22 \text{ g/cm}^3$  to  $2.84 \text{ g/cm}^3$ .

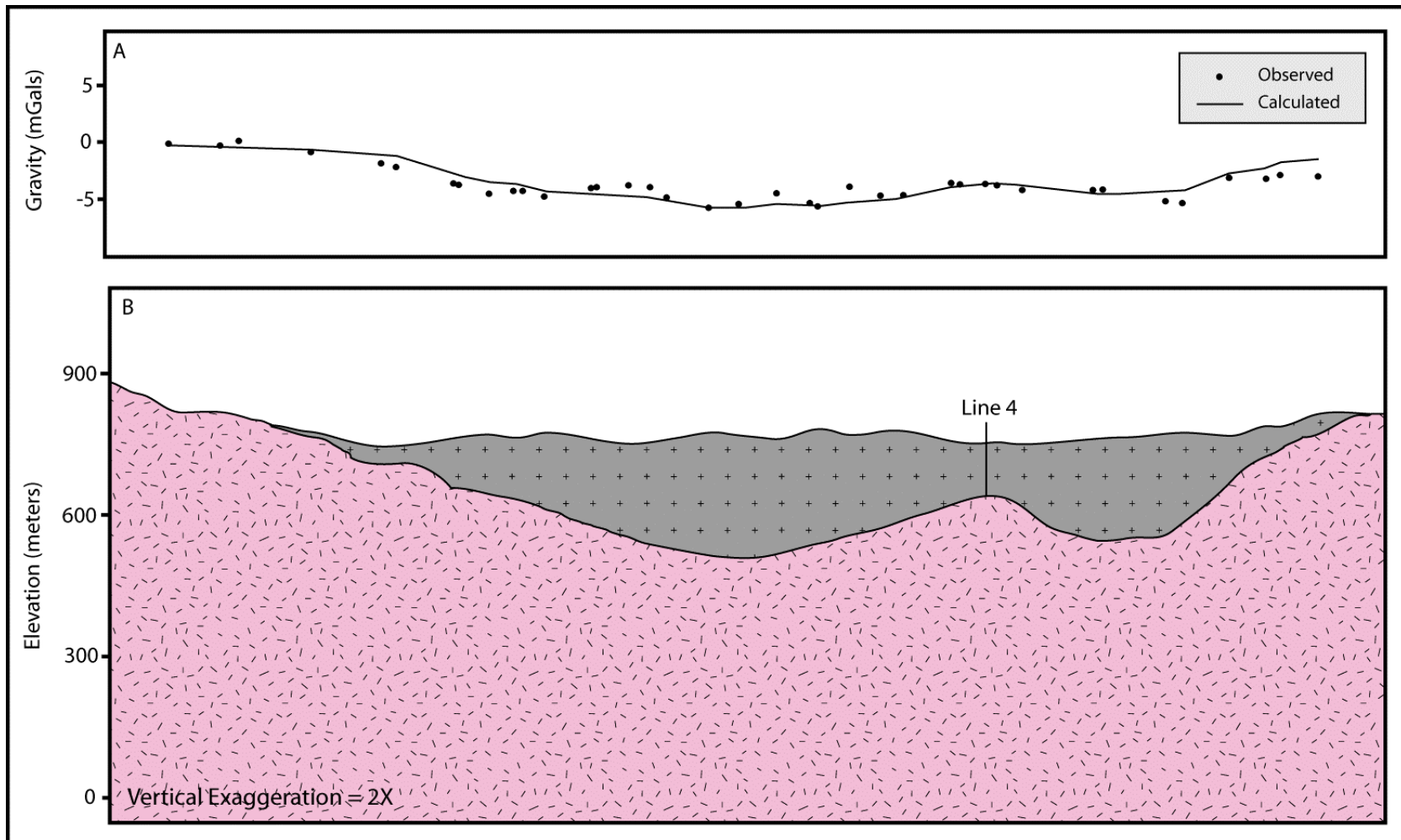


Figure 7. A mean density contrast model for Line 2 (Figure 9). A) The window above the geologic cross-section shows the response of the modeled gravity (black line) to the geometry of the two blocks. The black dots are the observed complete residual Bouguer anomalies. B) The gray polygonal block represents the mean density value fill  $\rho = 2.07 \text{ g/cm}^3$  and pink represents the basement complex  $\rho = 2.67 \text{ g/cm}^3$ . Elevation is with respect to the WGS84 ellipsoid. Vertical exaggeration is 2X.

#### **4.4 Gravity Line 1**

Line 1 is the northern-most east-west line in the Kamiak Gap, starting from Washington state highway 27 and running east along Mader Road to an outcrop exposure of pre-Cambrian quartzite on the western slope of Ringo Butte. This outcrop of basement provides a point of control for the observed gravity values for Line 1.

The interpretation of the subsurface geology beneath Line 1 (Figure 8) is based on the continuation of the high gravity anomaly extending from Ringo Butte and Angel Butte toward the intersection with Line 4. From Line 4 west toward highway 27 is a 2 km (1.25 mi) long channel filled with Palouse Loess, Wanapum basalt and Latah Formation sediments. The maximum depth to basement is in the center of this channel at a depth of 140 meters (450 feet) below the land surface. The best-fit model for Line 1 results in an error of  $\pm 4.5$  percent and does not permit the emplacement of the Grande Ronde basalt without compromising the geologic integrity of not just the model for Line 1, but for all the models tied together with Line 4 (discussed further in sections 4.7 and 4.8).

The most important implication of the interpretation of Line 1 is that the Grande Ronde basalt is not continuous through the Kamiak Gap, suggesting the existence of a barrier to ground water flow in the deep Grande Ronde aquifer system. This will be discussed later in section 5.

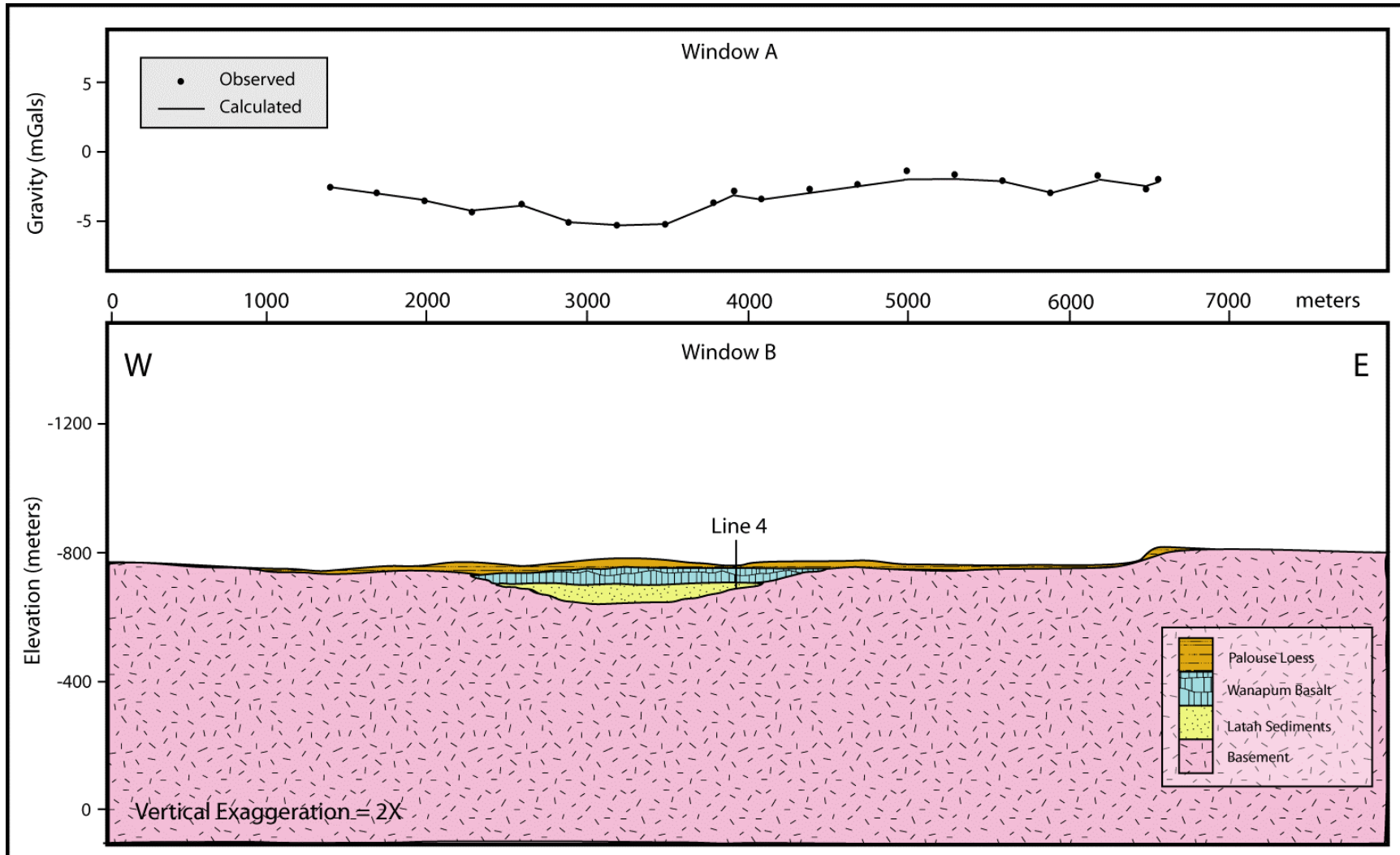


Figure 8. Gravity interpretation of Line 1. Window A shows observed gravity (dots) versus theoretical gravity (lines). Window B shows the marker labeled "Line 4" is where Line 1 intersects Line 4. Elevation is with respect to the WGS84 ellipsoid. Orthogonal to the cross-section is north; west is to the left and east is to the right. For a geologic explanation, refer to the legend. Vertical exaggeration of 2X.

#### **4.5 Gravity Line 2**

Line 2 traverses the middle of Kamiak Gap from bedrock on the eastern flank of Kamiak Butte to bedrock on the western slope of Angel Butte (Figure 9). The best fit of the theoretical gravity to the observed gravity results in a model error of  $\pm 4.2$  percent. This gravity model is constrained by two bedrock measurements at both ends of the survey line and from the tie-in point at the intersection with Line 4 to maintain an internal consistency of the geology. The interpretation of this gravity model shows a prominent basement drainage divide near the intersection with Line 4 that separates two pre-basalt channels, or valleys, from one another.

The maximum depth to basement of 270 meters (885 feet) from land surface is observed in the larger channel to the west of the basement topographic high (Figure 9); this is roughly 2.4 kilometers (1.5 miles) from the western end of Line 2. Interpretation of the materials contained in both bedrock channels includes the presence of low density Grande Ronde basalt overlain by an average thickness of 100 meters (330 feet) of Latah Formation sediments (i.e., the Vantage interbed). Overlying the Vantage interbed sediments are basalt of the Priest Rapids Member of the Wanapum Formation and loess of the Palouse Formation.

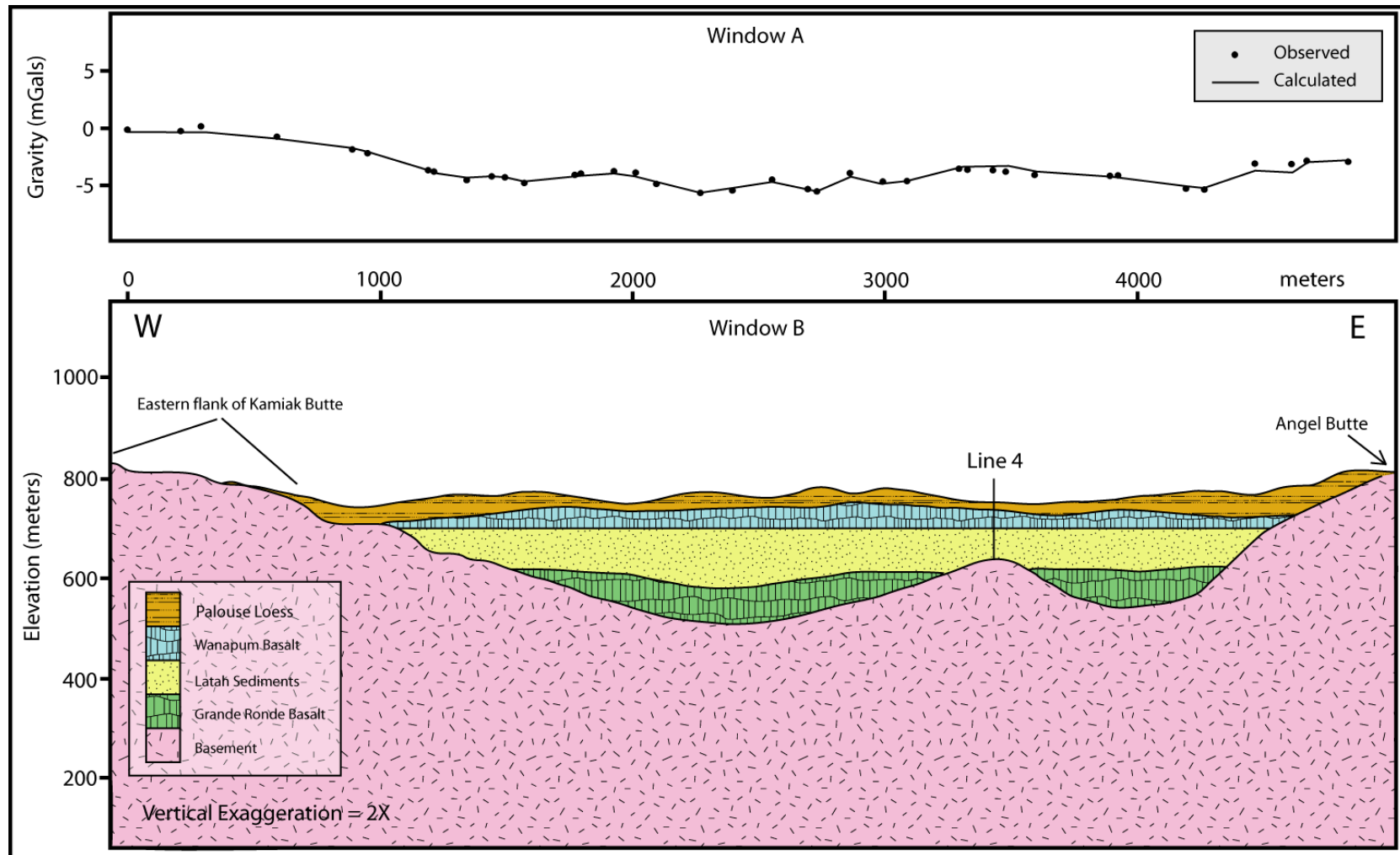


Figure 9. Gravity interpretation of Line 2. Window A shows observed gravity (dots) versus theoretical gravity (lines). Window B shows the intersection of Line 2 with Line 4 is indicated by the marker labeled “Line 4”. Angel Butte is indicated by the arrow. The eastern flank of Kamiak Butte is outlined to the left. North is orthogonal to the profile of the line, with west to the left and east to the right. Elevation is with respect to the WGS84 ellipsoid. Refer to legend for geologic explanation. Vertical exaggeration of 2X.

#### **4.6 Gravity Line 3**

The observed gravity measurements for Line 3 (Figure 10) are correlated to an estimated point of bedrock. Location of the bedrock is based on the extrapolation of information derived from a composite of the residual Bouguer anomaly contour map (Figure 5) and the geologic bedrock map presented in Figure 2. Gravity also was measured at a private well on West Road owned by Brock Hill for use as a point of control. However, the well does not contact the basement rock, nor does it penetrate beyond the upper three meters of the Latah Formation sediments. The well does provide control for the elevation of the top of the Priest Rapids Member, and the top of the Latah Formation sediments. The geologic interpretation of the gravity profile shows a narrow channel incised into the basement rock, filled with Grande Ronde basalt. Approximately 100 meters (330 feet) of Latah Formation sediments (i.e., Vantage interbed) overlie the Grande Ronde basalt in the central and eastern portions of this line; however, the thickness decreases to the west where the basement rock is closer to land surface. The Priest Rapids Member is exposed at the western end of Line 3 at the location of the local gravity base station used for the survey. The basalt is interpreted to maintain a near-constant thickness along the entire length of the line and to be juxtaposed with basement rocks on both ends. The Palouse Formation loess increases in thickness from near zero close to the gravity base station to substantial dune-like deposits in the eastern portion of the line.

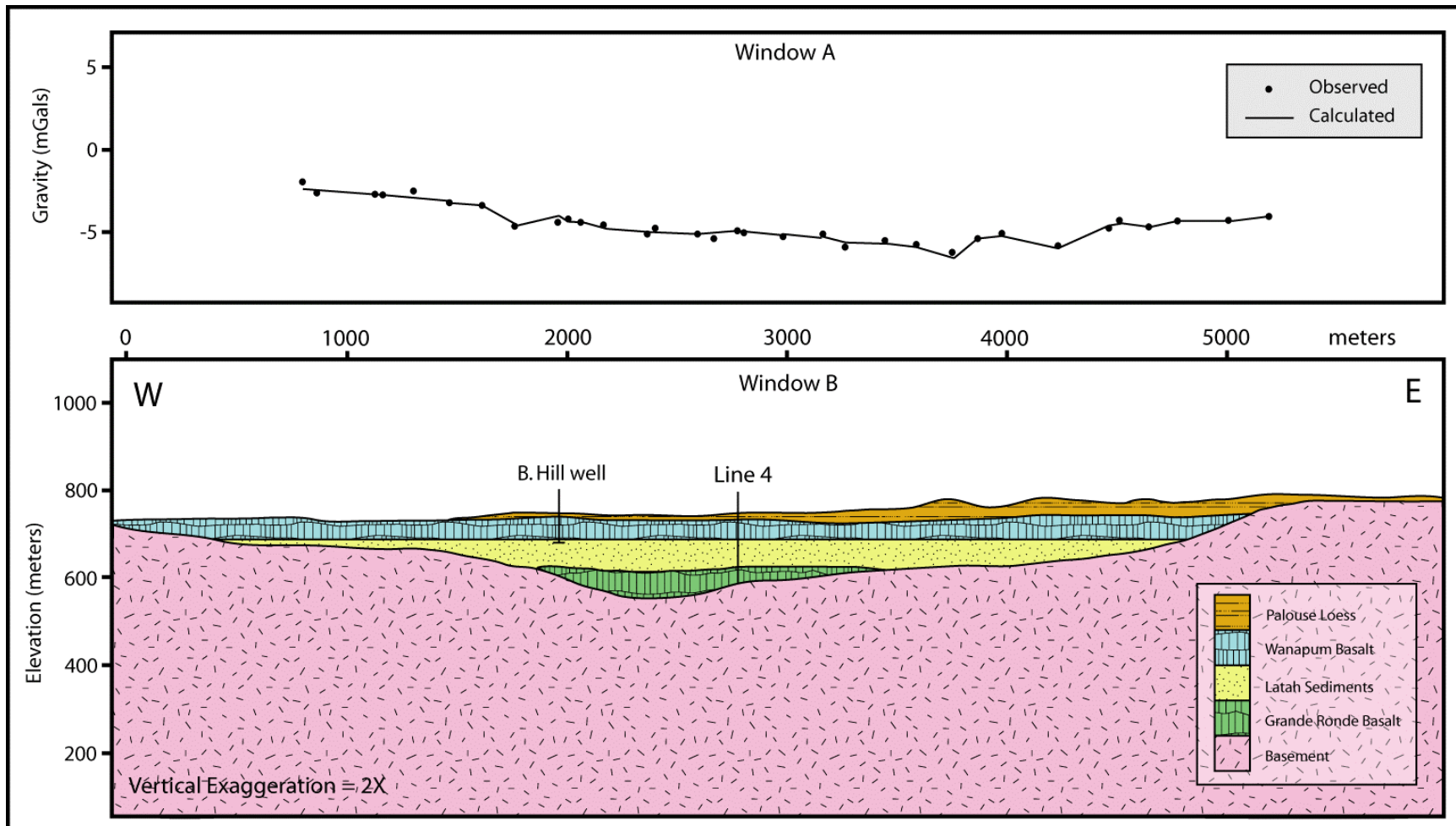


Figure 10. Gravity interpretation of Line 3. Window A shows observed gravity (dots) versus theoretical gravity (lines). Window B shows the intersection with Line 4 is indicated by the marker labeled “Line 4”. The marker labeled “B. Hill well” is the location of the well used to constrain the upper geologic units for the profile of this line. The well was completed in the upper sediments of the Latah Formation. Elevation is with respect to the WGS84 ellipsoid. Refer to the legend for geologic explanation. Vertical exaggeration of 2X.

#### **4.7 Gravity Line 4**

Line 4 (Figure 11) runs mostly northeast to southwest through the Kamiak Gap from Viola Road to the city of Palouse along private railroad tracks. In order to tie the three east-west lines together, common gravity stations were measured at each east-west gravity line intersection with Line 4. Having a north-south tie line brings the interpreted geology of all the other lines into conformity with one another. The only discrepancy in the geologic interpretations of the gravity measurements between Line 4 and the east-west lines is a 3-meter disagreement with the top of the Palouse Formation loess at the intersection of Line 2 and Line 4. The best-fit model of Line 4, after matching the geology of the east-west gravity lines, has an error of  $\pm 3.8$  percent.

The geologic interpretation of Line 4 consists of basement rock that ramps upward from the south and upward from the north to a saddle-like feature close to the intersection with Line 1. The Grande Ronde basalt abuts basement rock about halfway between the intersections with Line 2 and Line 3, making it discontinuous through the gap. Latah Formation sediments (i.e., Vantage interbed) that overlie the Grande Ronde basalt decrease in thickness from approximately 60 meters (200 feet) near the intersection of Line 4 with Line 3 to approximately 15 meters (50 feet) near the intersection of Line 4 with Line 1. From Line 1 north into Palouse, the Latah Formation sediments increase in thickness to about 60 meters (200 feet).

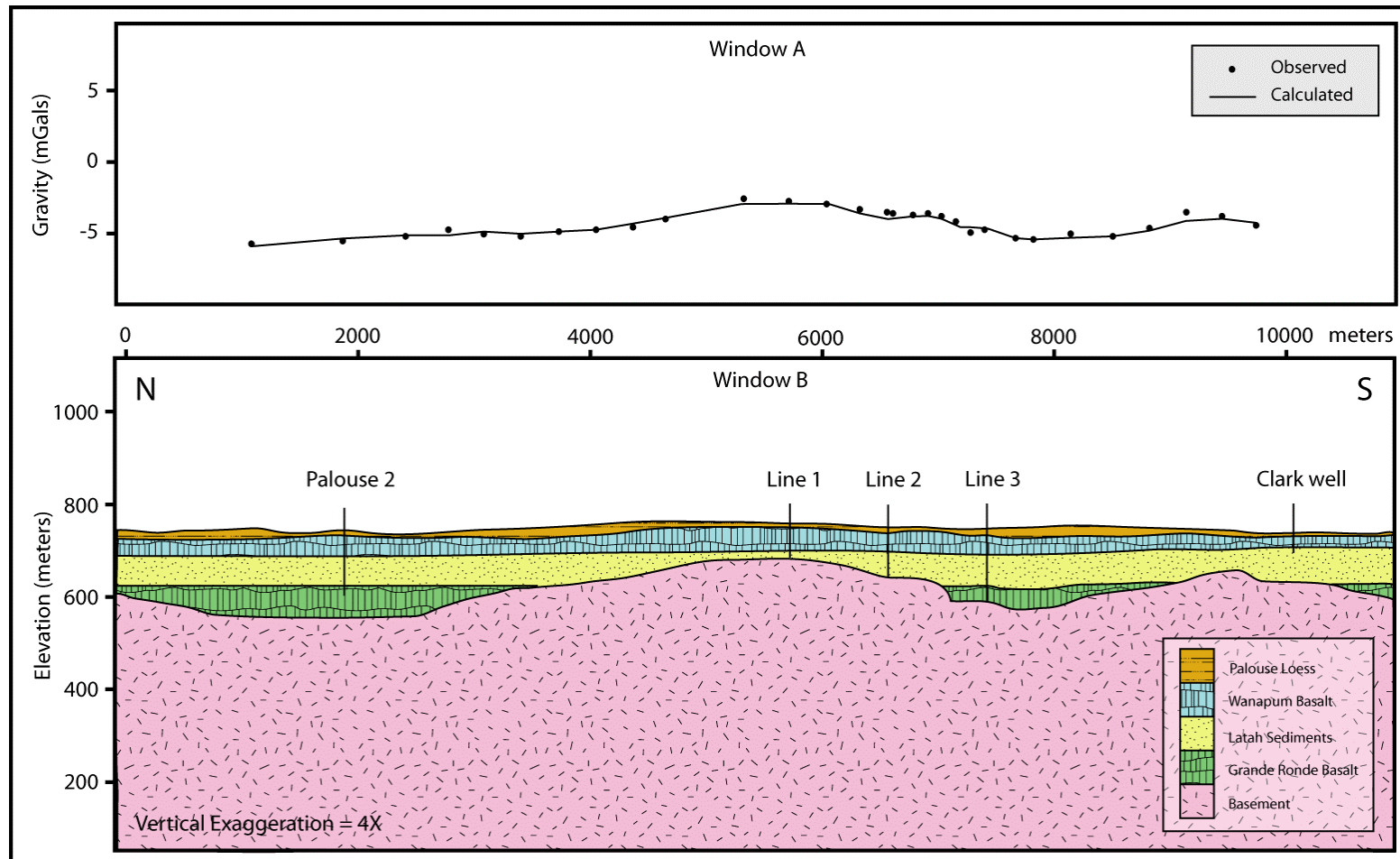


Figure 11. Gravity interpretation of Line 4. . Window A shows observed gravity (dots) versus theoretical gravity (lines). Window B shows the intersections with the other lines are indicated by the markers labeled, “Line 1”, “Line 2”, and “Line 3”. The marker labeled “Clark well” is the location of a well used to constrain the geology for the southern margin of the line. The bottom of the marker is the depth of well completion. The marker labeled “Palouse 2” is the location of the city of Palouse well #2, which was also used to constrain the geology. The bottom of the marker indicates well depth completion. Elevation is with respect to the WGS84 ellipsoid. Refer to legend for geologic explanation. Vertical exaggeration of 4X.

#### ***4.8 Conclusions from the Gravity Models***

The theoretical gravity models of the geology in the Kamiak Gap support the presence of a basement topographic high that effectively isolates the Grande Ronde basalt in the area of Palouse, Washington from the Grande Ronde basalt in Pullman and Moscow. Therefore, emplacement of the Grande Ronde basalt in the area surrounding Palouse must have occurred from the north side of Kamiak Butte as the flood basalts inundated the pre-basalt basement topography within the Palouse ground water basin. Latah Formation sediments that overlie the Grande Ronde basalt, range in thickness between 50 and 100 meters (160 and 330 feet) to the north and south of the Kamiak Gap, with the minimum thickness in the area of the basement topographic high near the intersection of Line 1 and Line 4, and along the edges of all bedrock hills. Basalt of the Priest Rapids Member of the Wanapum Formation is continuous through the Kamiak Gap, with an average thickness of about 60 meters (200 feet). The Palouse Formation loess covers the entire area and ranges in thickness from centimeters to tens of meters. A structural contour map of the subsurface basement is included in Appendix E.

## 5 Predictive Ground Water Model

### 5.1 Introduction

A numerical, finite-difference, ground water model of the Palouse ground water basin was created to predict the amount of water level decline (drawdown) that would be observed in Palouse, Washington from pumping wells in Moscow, Idaho. The purpose of the ground water model was to test the interpretations of the gravity models as to whether the Grande Ronde aquifer system is continuous through the Kamiak Gap from Moscow to Palouse. In order to do so, the ground water model simulates a real aquifer test conducted on January 31, 2006 (McVay, 2006). The aquifer test consisted of two pumping wells and nine observation wells. Moscow well #9 and University of Idaho well UI#3 were used as the pumping wells during the test. All other municipal and university wells were shut down for the duration of the test. The data collected during the aquifer test (McVay, 2006) were used to calibrate the model for values of hydraulic conductivity ( $K$ ) and specific storage ( $S_s$ ), as well as to compare the observed drawdown in Palouse with model predictions.

The ground water model was constructed using Visual MODFLOW™, which is a graphical interface software package developed by Waterloo Hydrogeologic™ that allows simulation of three-dimensional ground water flow and solute transport. The computational algorithm platform was developed by the U.S. Geological Survey (Harbaugh et al, 2000).

## 5.2 *Basic Model Conditions*

The ground water model was constructed in Visual MODFLOW Version 4.1. The model domain consists of a rectangular area of 140 km × 125 km (87 mi × 78 mi). The two-dimensional, finite difference model consists of grid composed of 353 x 315 cells with uniform cell spacings of  $\Delta x = \Delta y = 400$  m (1312 ft). The aquifer is modeled as a single layer, 400 m (1312 ft) thick (Figure 11). The grid is based on a UTM coordinate system. The extent of the model is sufficiently large so that grid perimeter boundaries do not influence water levels (<0.001 m) during the simulated aquifer test. The one-layer model has two zones, each with a different value for K. Zone 1 represents a homogeneous, isotropic confined aquifer with a constant K and  $S_s$ . Zone 2 represents impermeable, crystalline bedrock, forming boundaries to ground water flow. For the 1200-minute simulation, natural recharge and discharge were considered to be zero. The initial drawdown for the entire model was zero.

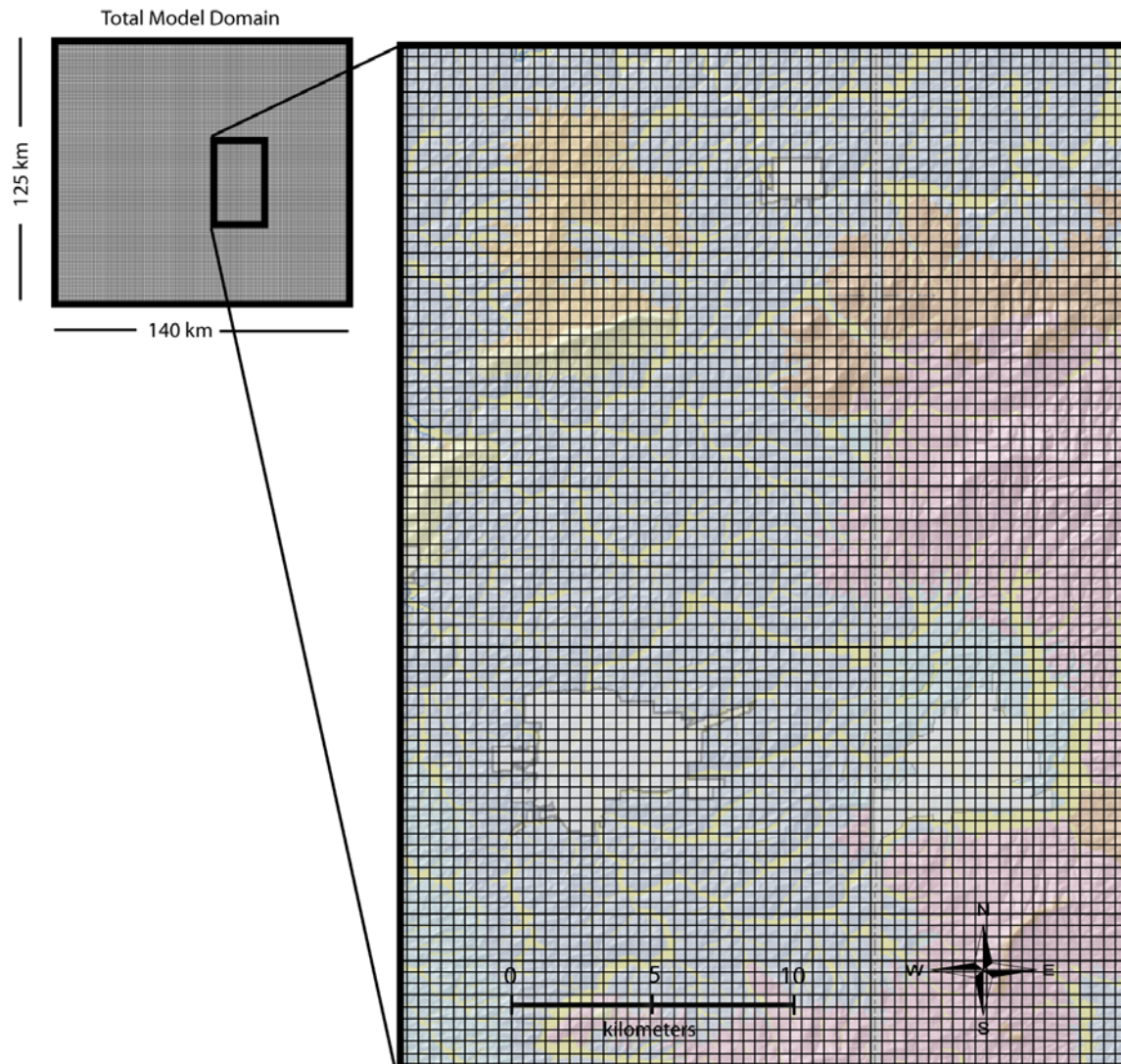


Figure 12. The ground water model domain, showing the grid. The extent of the model are in meters, projected in UTM NAD83 coordinates. The inner black rectangle is the area of interest shown in Figure 13 and Figure 15.

### 5.3 *Simulated Aquifer Test*

#### 5.3.1 *Real Aquifer Data*

Moscow #9 and UI#3 were chosen for the aquifer pump test, because municipal and university water needs required that they be pumped together; they are located 910 m (2985 ft) apart (Figure 13). The test started at 8:00 AM on January 31, 2006 with both wells pumping at full capacity. Moscow #9 pumped for 20 hours at a rate of 8540 lpm (2260 gpm) and UI#3 pumped for 6 hours at a rate of 8430 lpm (2230 gpm). During the

test, all other municipal and university wells (Washington State University and the University of Idaho) were shut down. Water level measurements were recorded in both city of Palouse wells #1 and #2, the Washington State Department of Ecology (DOE) well, and various private wells within the Palouse ground water basin. Those wells include: Brawdy, McGreevy, Naylor, Howell, Champion Electric and Central Premix. All well locations are identified in Figure 13.

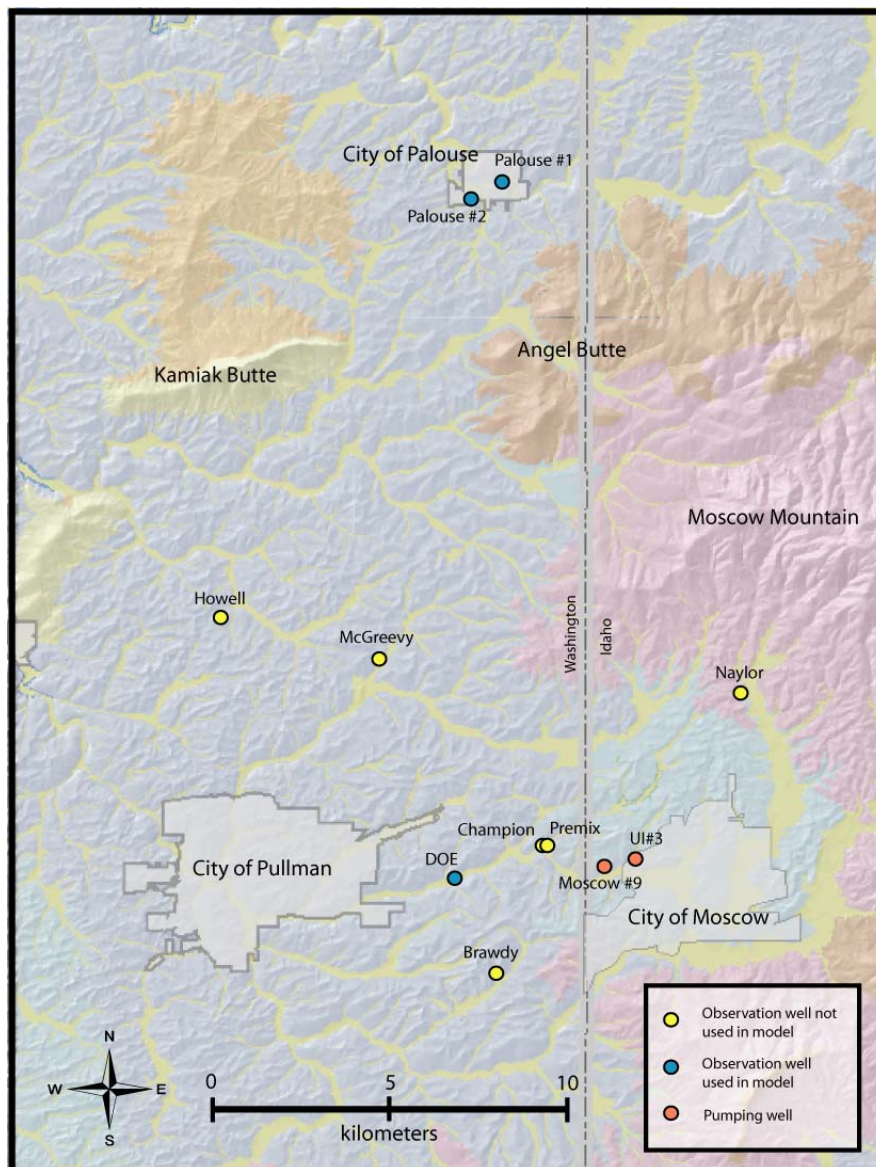


**Figure 13. Map of the area outlined in Figure 12, showing the locations of the two pumping wells and all the observation wells used in the aquifer pump test conducted January 31, 2006 (McVay, 2006).**

The water level measurements for the DOE well and Palouse #1 were recorded with pressure transducers that logged data on one-minute intervals. The pressure transducer installed in Palouse #2 is not capable of automatically recording water level measurements; therefore, water level measurements were recorded manually to the nearest tenth of a foot every 5 minutes from 4:30 AM to 7:00 PM on January 31, 2006. The change in barometric pressure was also recorded for the duration of the test to help explain any noticeable trends in the data. Figure 13 is a plot of observed drawdown in the DOE well, Palouse #1 and Palouse #2, and the change in barometric pressure in feet of water during the test. The pumping rates for Moscow #9 and UI#3 are plotted against the secondary y-axis.

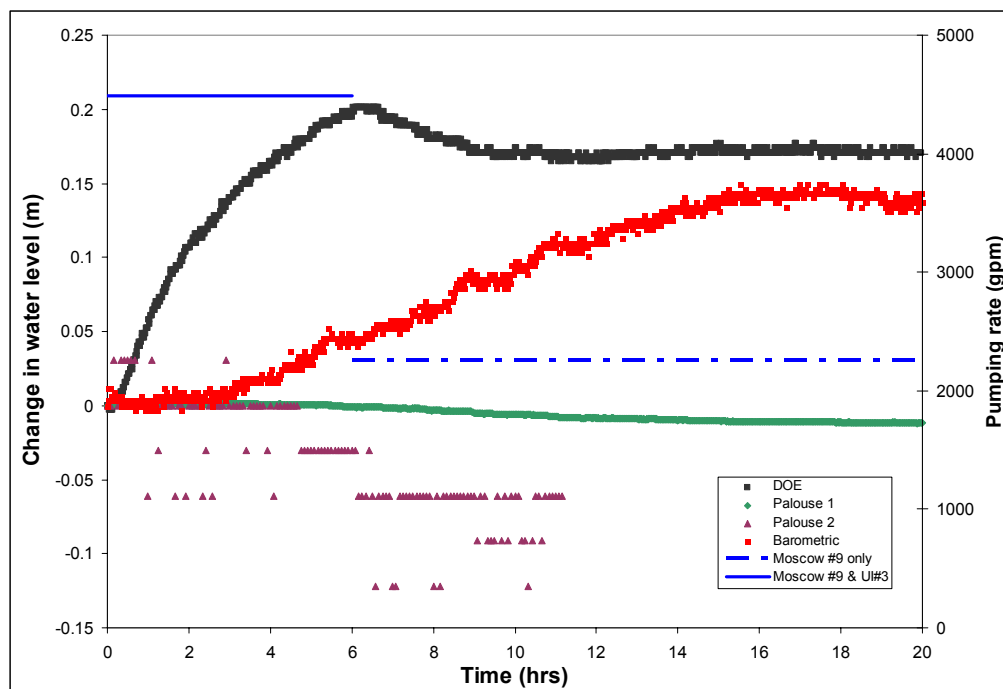


**Figure 14. Plot of the changes in water level for all wells used in the ground water model and the change in barometric pressure during the real aquifer pump test (plotted against the primary y-axis (left axis)). The pumping rates for Moscow #9 and UI#3 are plotted against the secondary y-axis (right axis). Time  $t = 0$  is the start of the aquifer test (8:00 AM). The solid blue line indicates duration of pumping for Moscow #9 and UI#3 combined. The dashed blue line indicates duration of Moscow #9 pumping after cessation of UI#3 pumping.**

#### 5.4 *Model Simulation*

To help in the development of boundary conditions for a MODFLOW™ model of the area, a base map of the geology created by Bush and Garwood (2005) (Figure 3) was imported from a geographic information system (GIS) software application. The base map is projected in NAD83 Zone 11 UTM coordinates. The geologic base map was used to trace low hydraulic conductivity boundaries along the areas of bedrock exposure in order to simulate approximate boundary conditions believed to exist in the Palouse ground water basin (Figure 15). The low K boundaries (Zone 2) were assigned a very low constant value of  $1 \times 10^{-25}$  m/day ( $3 \times 10^{-26}$  ft/day).

To simulate two pumping wells used in the real aquifer test, Moscow #9 and UI#3 were placed in the model according to their UTM positions. Both wells were simulated as fully penetrating pumping wells as follows: Moscow #9 pumped from time (t) = 0 to t = 20 hours at a rate of 8540 lpm (2260 gpm); UI#3 pumped from t = 0 to t = 6 hours at a rate of 8430 lpm (2230 gpm). Figure 15 also shows locations of the three observation wells added to the model, which include: DOE, Palouse #1 and Palouse #2. The real drawdown data were imported into the model for each observation well so that the real observed values of drawdown could be compared and analyzed with the predicted drawdown. Importing the real drawdown data into the model also allowed for model calibration and enabled the values for K and  $S_s$  to be estimated.

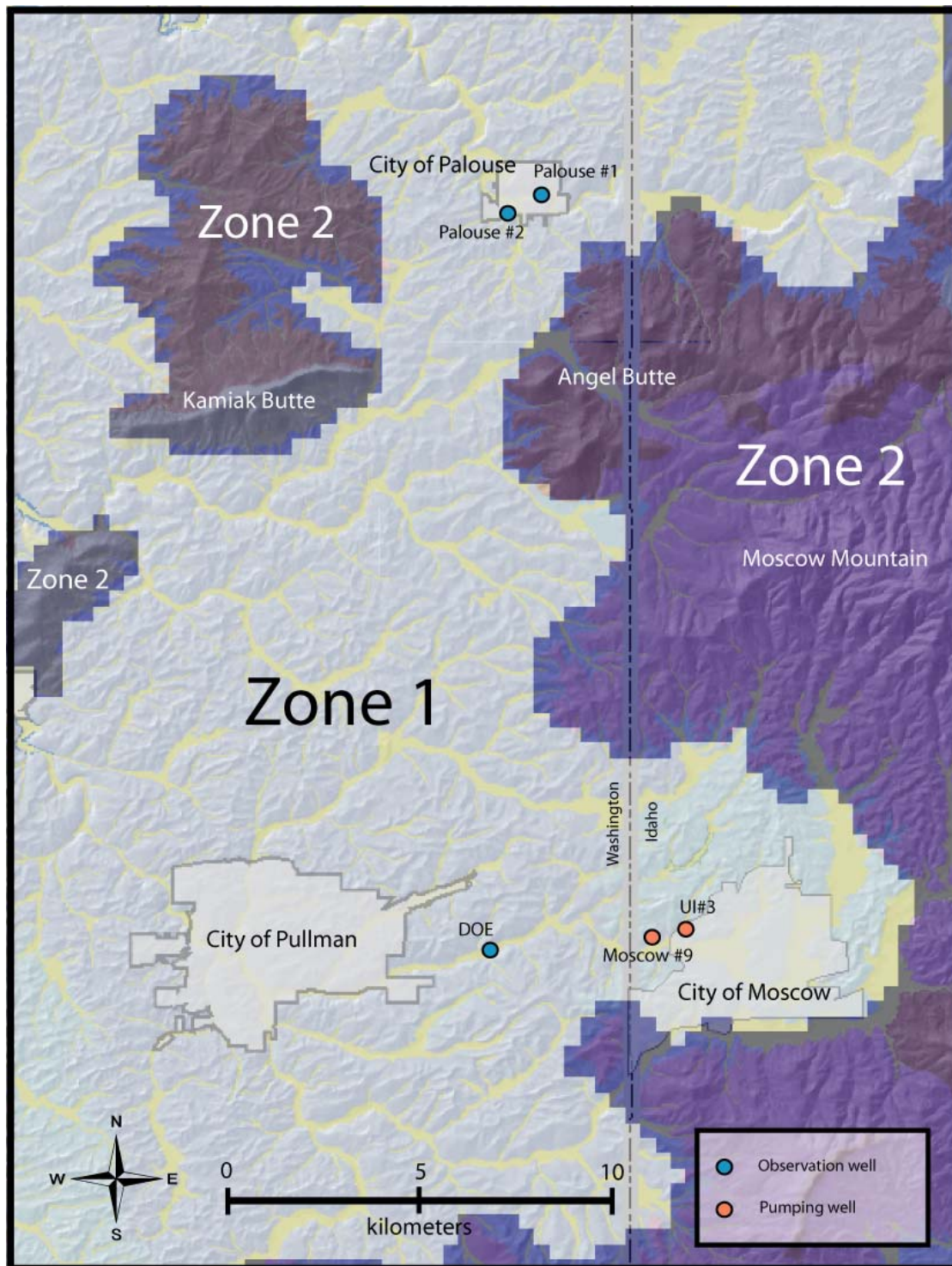


**Figure 15. Plan view of the ground water model outlined in Figure 12. The figure shows the wells used in the ground water model with respect to the mapped impermeable boundaries (dark regions labeled Zone 2).**

### 5.5 *Model Calibration*

Drawdown data for the DOE well were selected for use in calibration of the model to estimate values of  $K$  and  $S_s$ , because the drawdown data in this well showed the best theoretical response to pumping in Moscow (Figure 14). Arbitrarily chosen values for  $K$  and  $S_s$  were first used for model input data. Values for  $K$  and  $S_s$  were adjusted by trial and error, based on comparisons between the simulated drawdown for the DOE well and the real, measured drawdown data until a satisfactory match was achieved. If the predicted drawdown in the DOE well was less than the real observed measurements,  $K$  was decreased and the model was run again. When the slope of the predicted drawdown curve came close to matching the slope of the real drawdown data,  $S_s$  was changed and the model was run again. This process was repeated until the best fit of the predicted drawdown to the observed drawdown was obtained. Figure 16 shows the results of the calibration exercise.

The results of the model calibration yielded a  $K$  value of 195 m/day (640 ft/day) for Zone 1 and an  $S_s$  value of  $1.9 \times 10^{-7}$  /m ( $6.2 \times 10^{-7}$  /ft). Using these values, the aquifer test was simulated with two stress periods each divided into 25 time steps with a time-step multiplier of 1.2. Stress Period 1 extended from  $t = 0$  to  $t = 6$  hrs simulating discharge equal to the combined pumping rates of Moscow #9 and UI#3 (Figure 13). Stress Period 2 extended from  $t = 6$  hrs to  $t = 20$  hrs simulating only Moscow #9 pumping.

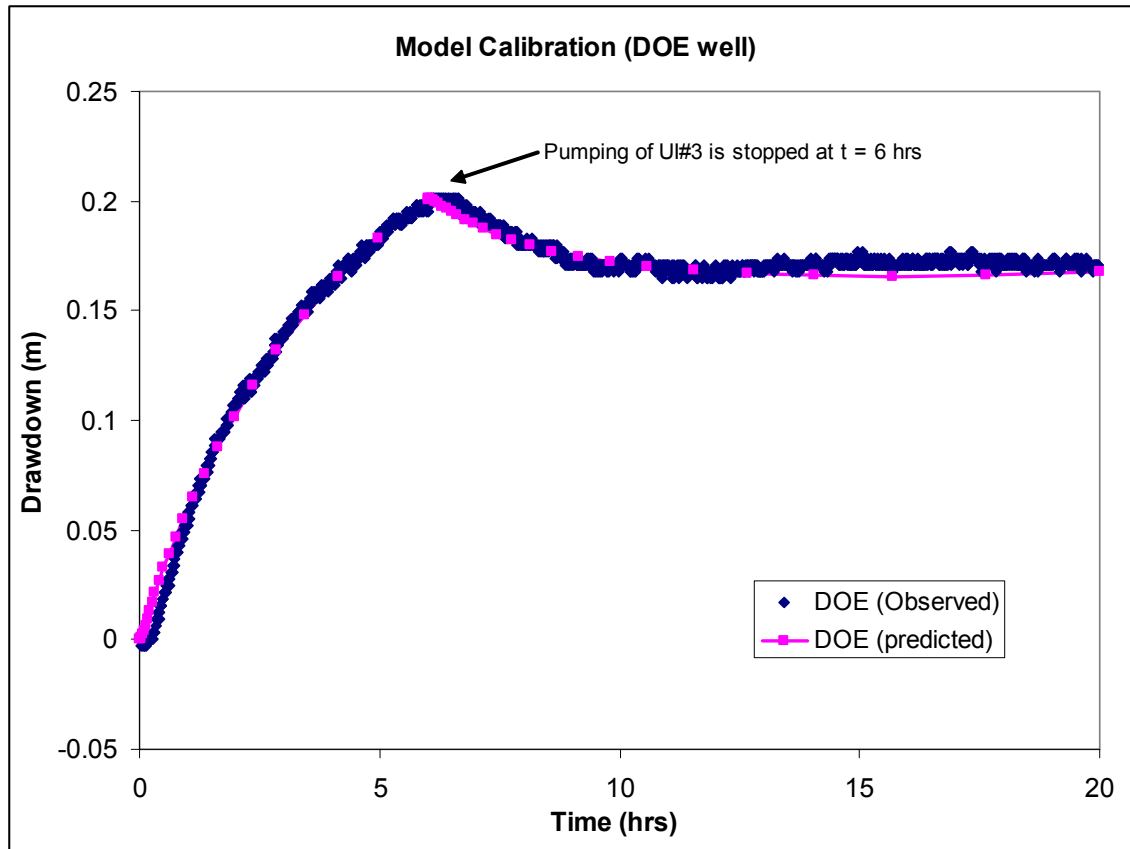


Figure 16. Plot of the results from model calibration. The magenta colored line and points represent the modeled drawdown. The blue colored points represent observed drawdown in the DOE well during the actual aquifer test. Time  $t = 0$  is the start of the real aquifer test at 8:00 AM on January 31, 2006 (McVay, 2006).

## 5.6 Results and Discussion

### 5.6.1 Palouse #1

In Figure 17, the observed drawdown data for Palouse #1 are compared with the simulated drawdown data generated in MODFLOW<sup>TM</sup>. At the end of the simulated aquifer test, the total, simulated drawdown in Palouse #1 is approximately 6 cm (0.2 ft). In contrast, the observed water level in Palouse #1 actually rose during the test, exhibiting a total water level rise of 1 cm (0.03 ft). A possible explanation for this water level rise is a drop in barometric pressure, which was observed during the real aquifer test (Figure 17). A drop in the barometric pressure can induce a water level rise in wells completed in confined aquifers (Freeze and Cherry, 1979).

Another explanation, but less likely, is the Noordbergum effect. The Noordbergum effect explains the phenomenon of water level rise during pumping by accounting for the compaction of the aquifer skeleton due to the withdrawal of water (Hsieh, 1997; Kim, 1997). When a confined aquifer is pumped, a certain magnitude of compaction of the aquifer skeleton occurs, which changes the porosity and hydraulic conductivity of the aquifer near the pumping well. MODFLOW™ is not capable of simulating the Noordbergum effect, because in order to do so, components of pore-elasticity need to be incorporated in to the model. Owsley (2003) first proposed the possibility of a hydraulic connection between Moscow and Palouse by the Noordbergum effect, when a water level rise in Palouse #2 was observed while pumping wells in Moscow.

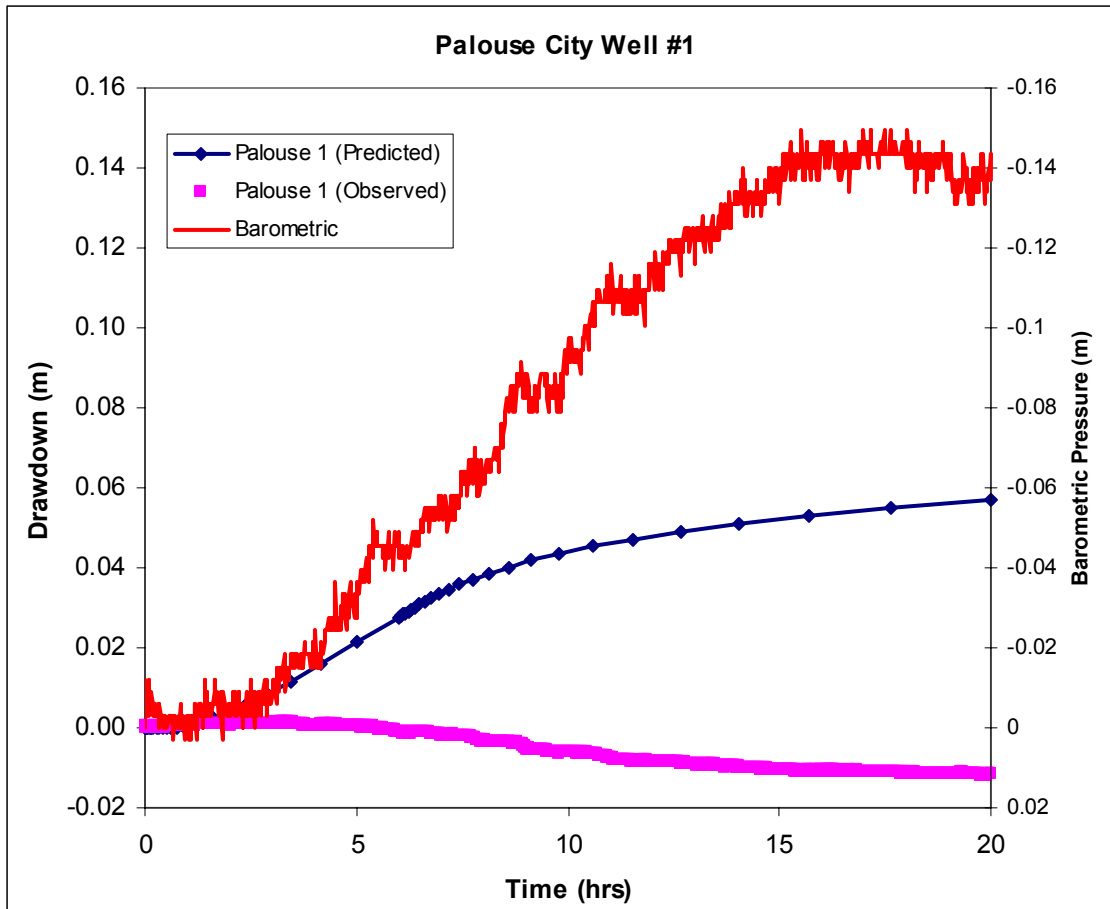


**Figure 17. Plot of the predicted drawdown versus the observed drawdown in Palouse well #1. Negative drawdown is water level rise in the well.**

### 5.6.2 Palouse City well #2

Figure 18 is a plot of the observed drawdown versus simulated drawdown for Palouse #2 for the duration of the aquifer test. The observed data were recorded manually for 11 hours after the start of the test. The data are much more scattered than the data for Palouse #1 because of the manner in which they were collected. However, it is clear that a water level rise occurred in Palouse #2 while pumping was taking place in Moscow. This may also be due to the significant drop in barometric pressure during the aquifer test. The predicted drawdown in Palouse #2 for the simulated test is the same as Palouse #1 of 6 cm (2.4 in). However, comparison of Figures 17 and 18 shows that the

magnitude of water level rise in Palouse #2 was much greater than in Palouse #1 during the aquifer test. The simulated drawdown for Palouse #2 is the same as Palouse #1 because the wells basically are located at the same location and distance from the pumping wells (19.3 km) (12.0 mi). Analysis of barometric effects on the real aquifer test data is beyond the scope of this investigation, and is discussed in detail by McVay (2006).

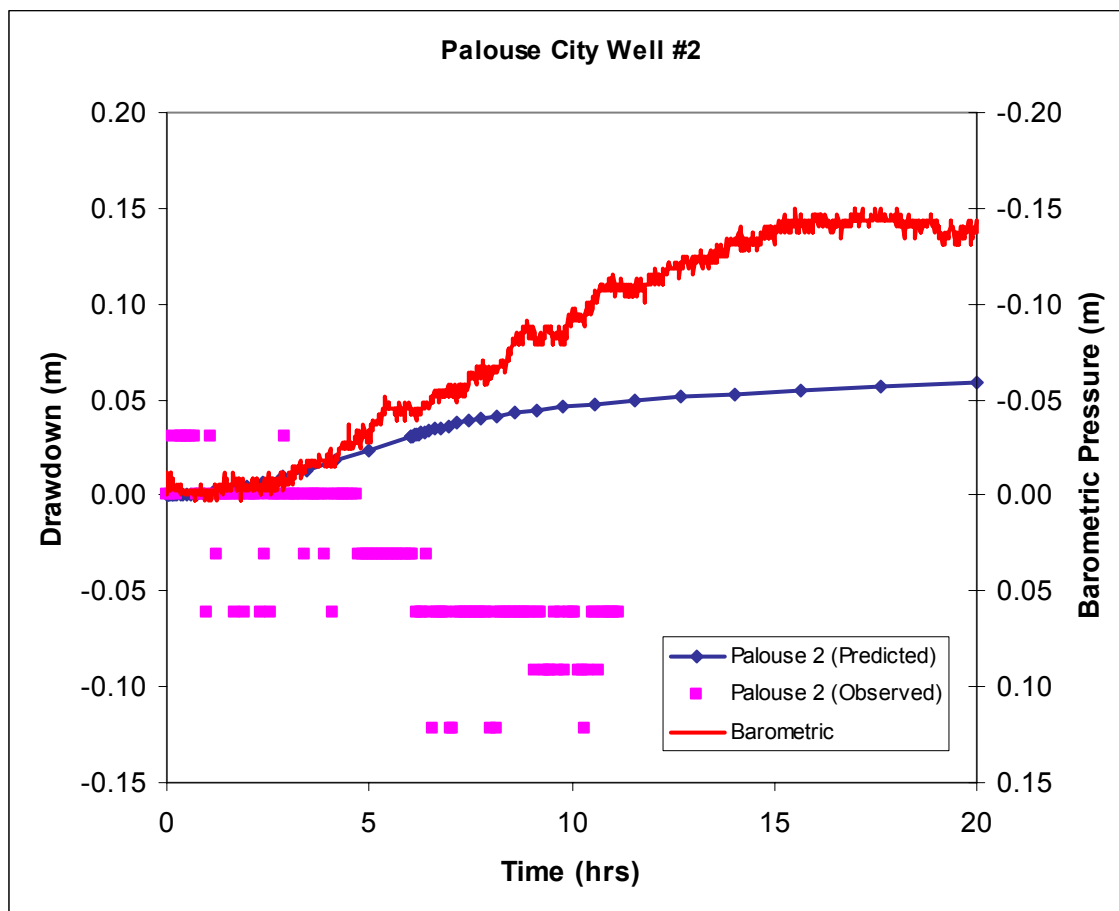


Figure 18. Plot of the predicted drawdown versus observed drawdown in Palouse well #2. Negative drawdown is water level rise in the well. Note: Drawdown is plotted on a different scale than in Figure 17.

## 6 Conclusions and Recommendations

Based on the real aquifer test simulated in the ground water model, about 6 cm (0.03 ft) of drawdown should have been expected in both Palouse wells #1 and #2. However, no drawdown was measured during the real aquifer test. The observed water level rises in both Palouse wells most likely can be explained by the drop in barometric pressure during the test. The lack of measurable drawdown in Palouse in response to pumping in Moscow provides supporting evidence (or at least no contradictions) to the interpretations of the subsurface geology based on the gravity models (i.e., discontinuity of the Grande Ronde aquifer system in the Kamiak Gap)..

### 6.1 Gravity model conclusions

The interpretation of the subsurface geology of the Kamiak Gap from the gravity models is that the continuity of the Grande Ronde Formation basalts is broken between the Moscow/Pullman area and the city of Palouse. The interpretations are based on the best fit of the east west gravity lines (e.g., Lines 1, 2 and 3) with the tie-in points on Line 4, logs for wells in the Kamiak Gap, and the bedrock measurements taken on the outcrop exposures on Kamiak Butte and Angel Butte.

The specific conclusions based on the gravity models are:

1. Gravity measurements are capable of delineating the sub-basalt basement topography in the Kamiak Gap.
2. Gravity measurements indicate that the maximum depth to basement rock in the Kamiak Gap is approximately 260 m (850 ft) below land surface along Line 2, 1.0 kilometers (0.62 miles) west from the intersection with Line 4.

3. The basement high modeled in Line 2 and Line 4 has a minimum depth of 76 m (250 ft) below land surface.
4. The gravity models show that the Grande Ronde Formation basalts are not continuous through the Kamiak Gap.
5. In the places where the modeled Grande Ronde basalts are present, the estimated elevation of the top of the Grande Ronde is from 580 m to 630 m (1900 ft to 2065 ft) above mean sea level.
6. The results of the gravity investigation suggest that ground water in the Palouse area likely flows parallel to the northern edge of Kamiak Butte, westward toward Colfax, Washington.

## **6.2 *Ground water model conclusions***

The specific conclusions based on the ground water model are:

1. The estimates of hydraulic conductivity (K) and specific storage ( $S_s$ ) for the Grande Ronde aquifer system are 195 m/day (640 ft/day) and  $1.9 \times 10^{-7}/\text{m}$  ( $6.2 \times 10^{-7}/\text{ft}$ ), respectively, based on the calibration of the model.
2. The ground water model suggests that measurable drawdown in wells Palouse #1 and Palouse #2 in response to pumping in Moscow is feasible if the same hydraulic properties that exist between wells Moscow 9, UI#3 and DOE also exist between Moscow and Palouse.
3. The maximum predicted drawdown for both Palouse city wells was 6 cm (0.03 ft) after 20 hours of pumping in Moscow.

4. The observed water levels in Palouse #1 and Palouse #2 rose during the aquifer pump test in a manner that appears to correlate with a drop in barometric pressure during that same time period.
5. The lack of definitive evidence for a hydraulic connection between Palouse and Moscow provides some supporting evidence for the interpretations of the gravity model that indicate the Grande Ronde basalts are not continuous through the Kamiak Gap.

### **6.3 Recommendations**

1. Drill a test well in the Kamiak Gap that intercepts the basement in the location of maximum depth to bedrock, to refine the subsurface geology, the gravity models and to refine our hydrogeological conception of the Palouse ground water basin.
2. Conduct aquifer pump tests with Pullman or Washington State University wells as the pumping center while monitoring the wells in Moscow, the DOE well, Palouse city wells #1 and #2, and private wells in order to verify the results of the ground water model.
3. Record water level measurements in private wells completed in the Latah Formation sediments within the Kamiak Gap while pumping in Moscow or Pullman to test for the Noordbergum effect.
4. After drilling a test well to bedrock, run seismic refraction lines in the Kamiak Gap to compliment gravity data and better constrain the loess/basalt contact; also run seismic reflection to better constrain the depth to bedrock

5. Update the old dataloggers for all municipalities and university wells to acquire more reliable, accurate water level measurements.
6. Determine accurate values for barometric efficiencies of Palouse #1 and Palouse #2 to be able to confidently correct for barometric trends in drawdown data.

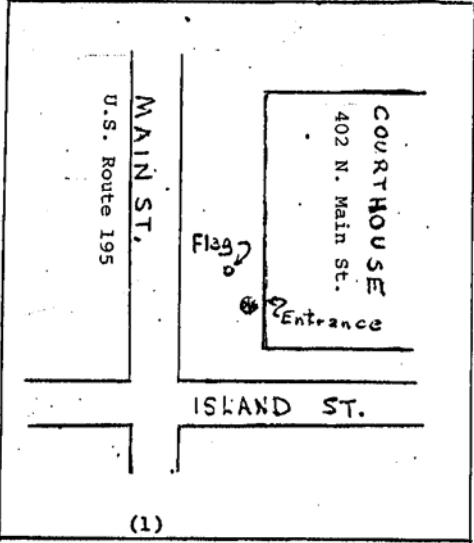
## 7 References

- Balco, G. and Stone, J.O., 2003, Measuring the density of rock, sand, till, etc. UW Cosmogenic Nuclide Laboratory, methods and procedures. <http://depts.washington.edu/cosmolab/chem.html> Accessed 3 February 2006.
- Bush, J.H., 1998a, Bedrock geologic map of the Moscow West quadrangle, Latah County, Idaho and Whitman County, Washington. Idaho Geological Survey: GM-23.
- Bush, J.H., 1998b, Bedrock geologic map of the Viola quadrangle, Latah County, Idaho. Idaho Geological Survey: GM-25.
- Bush, J.H., 2000, Bedrock geologic map of the Moscow East quadrangle, Latah County, Idaho. Idaho Geological Survey: GM-27.
- Bush, J.H., 2005, Personal communication.
- Bush, J.H., and Garwood, D., 2005, Unpublished geologic bedrock maps of the Albion, Elberton, Pullman, Palouse, Colfax North and Colfax South quadrangles. Geological Sciences Department, University of Idaho.
- Cogbill, Allen H., 1990, Gravity terrain corrections calculated using digital elevation models. *Geophysics* Vol. 55, No. 1, p. 102-106.
- Duncan, C., 1998, Geology of the Potlatch and Palouse 7½ - Minute Quadrangles, Idaho and Washington. M.S. Thesis. University of Idaho.
- Foxworthy, B.L., & Washburn, R.L., 1963, Groundwater in the Pullman Area Whitman County, Washington. Geologic Survey Water-Supply paper 1655
- Freeze, R.A., and Cherry, J.A., 1979, *Groundwater*. Englewood Cliffs, N.J.: Prentice-Hall.
- Gulick, C.W. 1994, Geologic Map of the Pullman 1:100,000 Quadrangle, Washington-Idaho. Washington Division of Geology and Earth Resources. Open File Report 94-6.
- Harbaugh, A.W., Banta, E.R., Hill, M.C., and McDonald, M.G., 2000, MODFLOW-2000, The U.S. Geological Survey Modular Ground-Water Model – User Guide to Modularization Concepts and the Ground-Water Flow Process. U.S. Geological Survey Open File Report 00-92, 130 p.

- Hildenbrand, T.G., Briesacher, A., Flanagan, G., Hinze, W.J., Hittelman, A.M., Keller, G.R., Kucks, R.P., Plouff, D., Roest, W., Seeley, J., Smith, D.A., and Webring, M., 2002, Rationale and Operational Plan to Upgrade the U.S. Gravity Database: U.S. Geological Survey Open-File Report 02-463, 12 p.
- Hinze, W., Aiken, C., Brozena, J., Coakley, B., Dater, D., Flanagan, G., Forsberg, R., Hildenbrand, T., Keller, G.R., Kellogg, J., Kucks, R., Li, X., Mainville, A., Morin, R., Pilkington, M., Plouff, D., Ravat, D., Roman, D., Urrutia-Fucugauchi, J., Véronneau, M., Webring, M., and Winester, D., 2003, New standards for reducing gravity observations: The Revised North American Gravity Database <http://paces.geo.utep.edu/research/gravmag/PDF/Final%20NAGDB%20Report%20091403.pdf> Accessed 2006 March 6.
- Hopster, Diane. 2003, A recession analysis of springs and streams in the Moscow-Pullman Basin. Master's thesis, Department of Geological Sciences, University of Idaho.
- Hsieh, P.A., 1997, Poroelasticity Simulation of Ground-Water Flow and Subsurface Deformation. U.S. Geological Survey Open File Report 97-47, 5 p.
- LaFehr, T.R., 1991, An exact solution for the gravity curvature (Bullard B) correction. *Geophysics* Vol. 56, No. 8, p. 1179-1184.
- Larson, Kathryn. 2000, Water resource implications of  $^{18}\text{O}$  and  $^2\text{H}$  distributions in a basalt aquifer system. *Ground Water* 38, p. 947-953.
- Lowrie, W. 2004, Fundamentals of Geophysics. Cambridge.
- Lum, W.E., Smoot, J.L., and Ralston, D.R., 1990, Geohydrology and numerical model analysis of ground-water flow in the Pullman-Moscow area, Washington and Idaho: U.S. Geological Survey Water Resources Investigations Report 89-4103, 73 p.
- McVay, M., 2006, personal communication.
- Kim, Jun-Mo and Parizek, Richard R., 1997, Numerical simulation of the Noordbergum effect resulting from groundwater pumping in a layered aquifer system. *Journal of Hydrology* 202, p. 231-241.
- King, R.A., Keller, C.K., & Schaumlöffel, J., 2000, Mechanisms of pesticide transport to surface water at the field scale in a dryland-agriculture region. State of Washington Water Research Center Report WRR-02, p. 1-23.
- Osiensky, J.L., 2006, personal communication.

- Owsley, D., 2003, Characterization of Grande Ronde aquifers in the Palouse Basin using large scale aquifer tests. M.S. Thesis. University of Idaho.
- Prieto, C., Perkins, C. and Berkman, E. 1985, Columbia River Basalt Plateau – An integrated approach to interpretation of basalt-covered areas. *Geophysics*, v. 50, no. 12, p. 2709 – 2719.
- Provant, A.P., 1995, The Geology and Hydrogeology of the Viola and Moscow West Quadrangles, Washington and Idaho. M.S. Thesis. University of Idaho.
- Saltus, R.W., 1993. Upper-crustal structure beneath the Columbia River Basalt Group, Washington: Gravity interpretation controlled by borehole and seismic studies: *Geological Society of America Bulletin*, v. 105, p. 1247-1259.
- Somigliana, C., 1930, Sul campo gravitazionale esterno del geoide ellissoidico: *Atti Reale Acad Naz Lin Rendi. Geofisica*, v 6, p. 237-243.
- Talwani, Manik and Ewing, Maurice, 1960, Rapid computation of gravitational attraction of three-dimensional bodies of arbitrary shape. *Geophysics*. Vol. 25, No. 1, p. 203-225.
- Telford, W.M., Geldart, L.P., & Sheriff, R.E., 1990, *Applied Geophysics*. Cambridge.
- Tolan, T.L., & Reidel, S.P. 1989, Revisions to the estimates of the areal extent and volume of the Columbia River Basalt Group. *Geological Society of America, Special Paper 239*, p. 1-20.
- WDOE, Washington Department of Ecology, <http://apps.ecy.wa.gov/welllog/> Accessed 6 March 2006
- Welch, A.H, Maurer, D.K., Lico, M.S., and McCormack, J.K., 2005, Characterization of surface-water quality in the S-Line Canal and potential geochemical reactions from storage of surface water in the basalt aquifer near Fallon, Nevada: U.S. Geological Survey Scientific Investigation Report 2005-5102, 52 p.

## Appendix A. Absolute Gravity Base Station COLFAX B

GRAVITY BASE STATION			
LATITUDE		STATION DESIGNATION	
46°53.0'N (1)		COLFAX B <i>1000000000</i>	
LONGITUDE		COUNTRY/STATE	
117°22.0'W (1)		USA/Washington	
ELEVATION		ADOPTED GRAVITY VALUE	
598.6 METERS (1)		g = 980 565. <del>44</del> mgals	
REFERENCE CODE NUMBERS		ESTIMATED ACCURACY	
DOD 0482-2		+ <del>100</del> mgals	
<del>0482-2</del>		DATE	
		MONTH/YEAR	
		February 1989	
DESCRIPTION AND/OR SKETCH			
<p>The station is located on the concrete sidewalk immediately beneath the bulletin board that is median between the two entrance doorways (southwest entrance) to the Whitman County Courthouse at the intersection of Main Street (U.S. Highway 195) and Island Street in downtown Colfax, Washington. The station is adjacent to USGS benchmark "U.S.G.S. 1965 S", which is located 14 inches below the ground near the entrance to the Courthouse. The station is directly beneath the lettering "1955" on the front wall (facing Main Street) of the Courthouse. (1)</p> <p>NOTE: The station was recovered as described by Daniel Winester, NOAA/NOS/NGS; 16 August 1988.</p> <p>Diagram revised by H. Fisher/DMAAC/DSGAA; February 1989.</p> 			
REFERENCE SOURCE			
(1) 3699			

GRAVITY STATION DESCRIPTION	STATION TYPE	STATION DESIGNATION
COUNTRY USA	State Base STATE/PROVINCE Washington	Colfax B CITY Colfax
LATITUDE 46° 53.'0 N 46.8833	LONGITUDE -117.3667 117° 22.'0 W	ELEVATION 598.6 Meters
GRAVITY STATION MARK None	AGENCY/SOURCE	INSCRIPTION
POSITION REFERENCE Map	POSITION SOURCE USGS 15'	SOURCE DESIGNATION Pullman
ELEVATION REFERENCE Benchmark	ELEVATION SOURCE USCGS	SOURCE DESIGNATION 1965 S
POSITION/ELEVATION REMARKS		
DESCRIPTION The station is located on the concrete sidewalk immediately beneath the bulletin board that is median between the two entrance doorways (southwest entrance) to the Whitman County Courthouse at the intersection of Main Street (U.S. Highway 195) and Island Street in downtown Colfax, Washington. The station is adjacent to USGS benchmark "U.S.G.S. 1965 S", which is located 14 inches below the ground near the entrance to the Courthouse. The station is directly beneath the lettering "1955" on the front wall (facing Main Street) of the Courthouse.		
DIAGRAM/PHOTOGRAPH		
DATE OF PHOTO		
DESCRIBED BY J. F. Lambert	AGENCY AMS	DATE Sept 1967

TPC FORM 115-29  
MAY 70

REPLACES TEST EDITION, AUG 69, WHICH IS OBSOLETE

## **Appendix B. Gravity Spreadsheet Paper/Spreadsheet Instructions**

**Gravity reduction spreadsheet to calculate the Bouguer anomaly using standardized methods and constants**

**Derek I. Holom and John S. Oldow**

*Department of Geological Sciences, University of Idaho, Moscow, Idaho 83844-3022,  
USA*

### **ABSTRACT**

**Current standards for reduction of observed gravity to a modeled Bouguer anomaly largely are unregulated and vary among geophysical textbooks, commercial software programs, and academic research spreadsheets available for download from the internet. Using new standards established by the U.S. Geological Survey and the North American Gravity Database Committee, we developed a spreadsheet for reduction of raw data to the Bouguer anomaly and with the use of terrain correction the Complete Bouguer anomaly. The reduction is based on ellipsoidal height. Included in the data reduction package is a U.S. Geodetic Survey transformation program that enables restoration of orthometric height readings (typical of legacy data) to ellipsoidal height. The spreadsheet is available for free download at [geongrid.org](http://geongrid.org). We view the spreadsheet as particularly useful for field data reduction and modeling where internet access is limited or unavailable.**

**Keywords: Bouguer, Bouguer anomalies, gravity, gravity anomalies, gravity methods, spreadsheets.**

## **INTRODUCTION**

With the use of the Global Positioning System (GPS) for surveying station locations and elevations, availability of digital terrain models, and enhanced computational capability, gravity modeling is a cost-effective tool in subsurface analysis ranging from basin to continental scale studies. Existing gravity data for North America are archived and readily accessible via the internet at the Pan-American Center for Earth and Environmental Studies website (<http://paces.geo.utep.edu/>). The North America gravity database provides principal facts and Free Air and Bouguer anomalies calculated by a FORTRAN algorithm based on preferred correction and anomaly equations established by the Standards/Format Working Group of the North American Gravity Database Committee (Hinze et al., 2002).

To facilitate adoption of the standards established by the North American Gravity Database Committee (Hinze et al., 2002) by the research community and to provide an easy to use, portable gravity correction and anomaly computation platform, we developed a gravity spreadsheet. The spreadsheet is based on Microsoft Excel, which is a common software application used by government agencies, research institutions, and private companies. The equations used in the spreadsheet are derived from the FORTRAN code written by Mike Webring of the U.S. Geological Survey and are the same as those used

by the GeoNet Server at the Pan-American Center for Earth and Environmental Studies (PACES, 2006).

## STANDARDIZED GRAVITY REDUCTION

The equations described in this section are used in the gravity spreadsheet and conform to the new gravity standards set by the U.S. Geological Survey (Hildebrand, 2002) and the Standards/Format Working Group of the North American Gravity Database Committee (Hinze et al., 2003).

### Ellipsoid Theoretical Gravity

The ellipsoid theoretical gravity calculation uses the Somigliana closed-form formula based on the 1980 Geodetic Reference System (GRS80) to predict the gravity at any latitude  $\varphi$  north or south (Hildebrand, 2002).

$$g_{\varphi} = g_e \frac{1 + k \sin^2 \varphi}{\sqrt{1 - e^2 \sin^2 \varphi}} \quad (1)$$

where values for the GRS80 reference ellipsoid are:  $g_e = 978032.67715$  mGals,  $k = 0.001931851353$  is a dimensionless coefficient,  $e^2 = 0.0066938002290$  is a dimensionless coefficient

### Atmospheric Correction

The mass of the atmosphere is unaccounted for in the theoretical gravity calculation and must be subtracted from the observed gravity. The atmospheric correction uses the height  $h$  of the gravity station in meters above the GRS80 ellipsoid in the following equation (Hildebrand, 2002):

$$g_{atm} = 0.874 - 9.9 \times 10^{-5} h + 3.56 \times 10^{-9} h^2 \quad (3)$$

### Height Correction

Measurements of observed gravity decrease with increasing distance from the center of the Earth. In order to be compared with the theoretical gravity at the same location, the height of the gravity station must be corrected to the reference ellipsoid (Hildebrand, 2002):

$$g_h = -(0.3087691 - 0.0004398 \sin^2 \varphi)h + 7.2125 \times 10^{-8} h^2 \quad (4)$$

where,  $h$  is the height of the gravity station in meters above the GRS80 ellipsoid and  $\varphi$  is the latitude of the gravity station

## Bouguer Spherical Cap

The Bouguer spherical cap correction sets the observed gravity value to a standard density based on either the average density of the continental crust ( $2.67 \text{ g/cm}^3$ ) or to a site specific average density of the basement rock for local surveys. Older methods of reducing gravity data used a similar correction called the Bouguer slab, which was based on a flat Earth model. The Bouguer spherical cap correction is the new standard formula that accounts for the curvature of the Earth (Hildenbrand, 2002).

$$g_{sc} = 2\pi G\rho(\mu h - \lambda R) \quad (5)$$

where  $\mu$  and  $\lambda$  are dimensionless coefficients (LaFehr, 1991),  $G$  is Newton's gravitational constant =  $6.6725985 \times 10^{-11} \text{ m}^3 \text{ kg}^{-1} \text{ s}^{-2}$ ,  $\rho$  is the density of the spherical cap, usually  $2670 \text{ kg m}^{-3}$ ,  $h$  is the height of the gravity station above the GRS80 reference ellipsoid (km), and  $R$  is the combined height of the gravity station and average radius of the Earth (km).

## GRAVITY SPREADSHEET

The gravity spreadsheet calculates the corrections for instrument drift, latitude, height above the GRS80 reference ellipsoid, atmospheric, and the Bouguer spherical cap, as well as the DC shift for multiple day gravity surveys. The meter-specific calibration

table in the spreadsheet will convert LaCoste-Romberg G-model gravimeter counter readings to corrected gravity measurements. Tide and terrain corrections are not calculated in the spreadsheet, but users can enter values from other programs, such as InnerTC (Cogbill, 1990) in order to reduce gravity data to Bouguer anomalies.

Prior to the recent standards set by the U.S. Geological Survey, typical gravity reduction has used orthometric heights (i.e., elevation with respect to mean sea level, or the geoid) to calculate Free-air and Bouguer slab corrections. The free-air correction, now called the height correction (Hildebrand, 2002), will be equal to zero at the altitude of the GRS80 ellipsoid, rather than at sea level.

To compensate for the difference between the ellipsoid and the geoid, the indirect effect is an additional correction added to the gravity data reduction in order to calculate the Bouguer anomaly. The revised methods presented in this paper and implemented in the spreadsheet, use the height of the gravity station with respect to the GRS80 reference ellipsoid, which eliminates the need for the indirect effect as described by Hinze et al (2003) and Hildebrand (2002). To calculate the indirect effect, the user must find the height of the geoid separation, which effectively finds the height of the ellipsoid; therefore, the user can omit the unnecessary step of calculating the indirect effect by using the ellipsoidal height in the first place.

### **Input Parameters**

The four basic input parameters needed to calculate a Bouguer anomaly in the gravity spreadsheet include: 1) the height of the gravity station above the GRS80

reference ellipsoid, 2) the latitude of the station in WGS84 coordinates, 3) the drift and tide corrected observed gravity readings tied to an absolute gravity base station, and 4) the terrain correction for the location of the gravity station.

The more advanced calculations built into the spreadsheet include: 1) the instrument drift correction, 2) latitudinal correction, 3) LaCoste-Romberg gravimeter reading conversions, 4) DC shift, and 5) conversion from local observed gravity to absolute gravity readings. Refer to Appendix A for a detailed description of how to use the spreadsheet for optimal use.

### **Error Analysis**

In order to benchmark the equations in the gravity spreadsheet converted from the U.S. Geological Survey FORTRAN code, gravity data available from the GeoNet server were entered into the gravity spreadsheet for an error analysis. The difference between the Bouguer anomalies calculated by the GeoNet server and the gravity spreadsheet results in a range of error from 2 to 14  $\mu\text{Gals}$  (i.e., 0.002 to 0.014  $\text{mGals}$ ). The range of errors was plotted against all the corrections used in the spreadsheet and shows no discernible pattern to indicate the cause of error; the difference is most likely due to a truncation error in the spreadsheet program. For the sake of redundancy, figure 1 is a scatter plot that shows the random pattern of the error versus two of the corrections used in the spreadsheet.

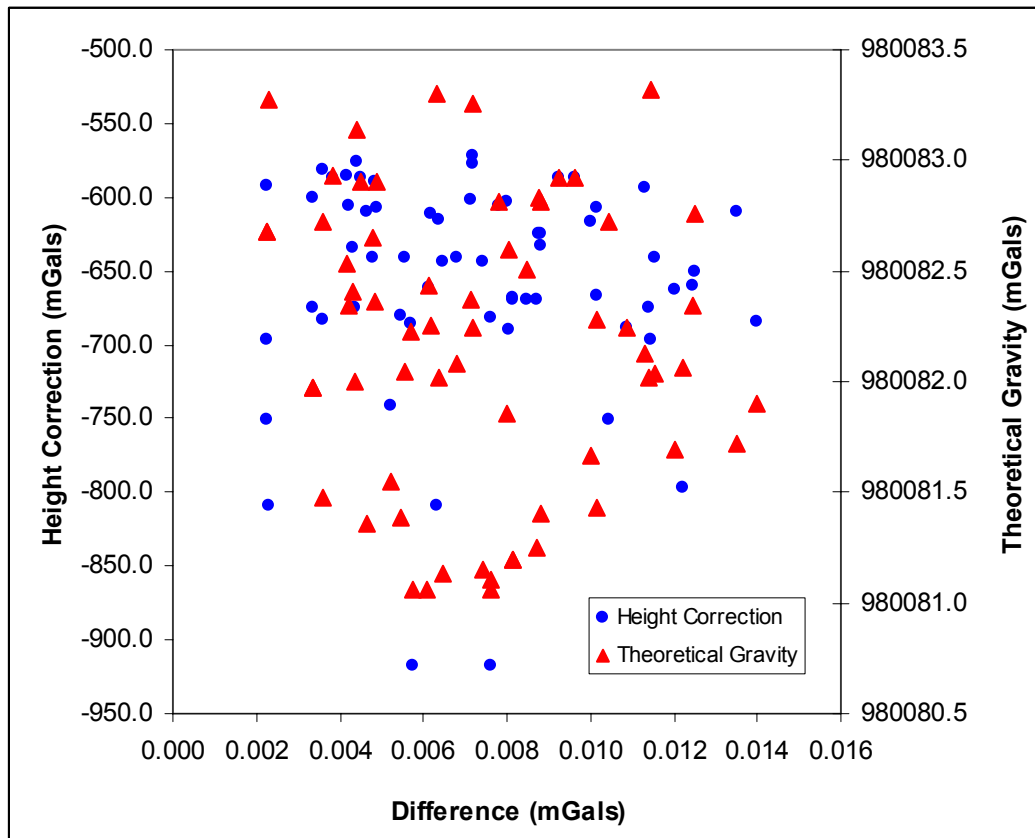


**Figure 19. Scatter plot of the difference of Bouguer anomalies between the gravity spreadsheet and the values downloaded from the GeoNet server.**

The Bouguer anomaly values downloaded from the GeoNet server were calculated using orthometric heights and can result in an error as much as  $\pm 7$  mGals, because the separation of the geoid from the ellipsoid on the North American continent can be as great as  $\pm 20$  meters. If using the gravity data downloaded from the GeoNet server with local gravity data, the heights of each station need to be recalculated using the NGS transformation software INTG provided with the gravity spreadsheet. INTG is a program developed by the United States government that uses the 2003 geoid model to calculate the geoidal separation (NGS, 2006).

## CONCLUSIONS

The gravity spreadsheet is free and provides a simple tool for the reduction of raw gravity data to Bouguer anomalies, all in conformity with the standards set by the USGS and the North American Gravity Database Committee. The spreadsheet eliminates the need for internet access by allowing the user to calculate the Bouguer anomaly of a gravity station within minutes of acquisition.

## APPENDIX A:

### GRAVITY SPREADSHEET v.1.0 INSTRUCTIONS

Each column in the gravity worksheet of the Gravity Spreadsheet v.1.0 workbook is described below, including the purpose of the column and its associated formula; original equations are given in case the spreadsheet is modified.

#### **Column A: *Gravity Station***

Gravity station identification.

#### **Column B: *Date***

Enter the date as MM/DD/YYYY. Calculations for time durations use this format.

#### **Columns C and D: *Time – Hours/Minutes***

Enter hours in military time. It is important use the 0-24 hour time scale because subsequent calculations depend on this format.

**Column E: *Duration (hours)***

This equation calculates the time, in decimal hours, that has elapsed from the initial base station reading. These calculations are used to determine the drift correction.

$$E3 = ((B3 - \$B\$3) * 24) + ((C3 + (D3/60)) - (\$C\$3 + (\$D\$3/60)))$$

**Columns F – K: *Latitude and Longitude***

Under both headings are three columns: d – degrees; m – minutes; sec- seconds. If your coordinates are already in decimal degrees skip this data input section.

**Column L and M: *Latitude and Longitude (DD)***

DD stands for decimal degrees. These columns convert coordinates that are in degrees, minutes and seconds into decimal degrees.

$$L3 = F3 + (G3/60) + (H3/3600)$$

$$M3 = -1 * (I3 + (J3/60) + (K3/3600))$$

**Column N: *Ellipsoid Height (m)***

Enter altitude of gravity station in meters based on the GRS 80 ellipsoid. If altitudes of gravity stations are orthometric you will need to use a geoid height separation calculator to convert to ellipsoidal heights. The INTG.exe\* program was created by the National Geodetic Survey for calculating the geoid separation and is included in the Holom-Oldow Gravity Reduction package.

---

\* INTG.exe is the property of the government of the United States of America.

**Columns O and P: Orthometric Height (m) and Geoid Hgt Separation (m)**

Enter orthometric height values in *Column O* and the geoid separation in *Column P*. In *Column N*, enter the equation: =O3+P3

**Column Q: Lat Degs to Km**

This column converts latitudinal difference between the gravity station and the absolute gravity base station to kilometers poleward. The equation uses a look-up function to find the appropriate conversion factor from the table in the “Lat-km” worksheet. The values calculated in this column are used for latitude corrections.

$$Q3=(\textit{Absolute Base}!\$B\$3-L3)*(VLOOKUP(L3,\textit{Lat-km}!\$A\$1:\$B\$11,2))$$

**Columns R and S: Counter and Calibrated (mgal)**

These two columns are used to calibrate the counter values from a LaCoste-Romberg gravity meter. Each gravity meter has a specific calibration table which the user should manually input into “Calib. Table” worksheet. *If the newly entered table is longer or shorter than the original, then make sure to change the cell range in the equation under **Calibrated** column. (e.g. if the calibration sheet supplied with the LaCoste and Romberg gravity meter happens to have one more row than the calibration sheet for the G-1069 meter, change the following equation from:*

$$S3=(R3-VLOOKUP(R3,\textit{Calib. Table}!\$A\$5:\$C\$75,1))*(VLOOKUP(R3,\textit{Calib. Table}!\$A\$5:\$C\$75,3))+VLOOKUP(R3,\textit{Calib. Table}!\$A\$5:\$C\$75,2)$$

To:

$$S3 = (R3 - VLOOKUP(R3, 'Calib. Table'!$A$5:$C$76, 1)) * (VLOOKUP(R3, 'Calib. Table'!$A$5:$C$76, 2) + VLOOKUP(R3, 'Calib. Table'!$A$5:$C$76, 3))$$

The equation to calibrate the counter values uses three lookup commands to find the associated factor intervals and cumulative values for the specific counter values entered in the **Counter** column.

**Column T: *Measured (mgal)***

The digital gravity reading from a LaCoste-Romberg gravimeter is entered in this column (mGals). If the gravity data being entered is already in relative observed gravity readings, skip this column and move on to the Observed Gravity column *U*.

**Column U: *Observed Gravity (mGals)***

This column is the summation of the columns *S* and *T*. If the user is entering the data from a Scintrex gravimeter, then skip columns *S* and *T* and enter the observed values straight into column *U*.

**Column V: *Tide (mgal)***

The user must make earth tide corrections using another program, because they are not calculated in this spreadsheet. Enter the earth tide values for the specific time and location of each gravity measurement.

**Column W: *Tide Corrected (mgal)***

This column is the summation of the **Calibrated, Measured** and **Tide** columns. Values in this column are used to make the drift correction.

$$W3 = V3 + U3$$

**Column X: Drift (mgal/hr)**

The drift correction uses the base station gravity measurements, before and after the survey, to equate the rate of drift for the gravity measurements during the survey.

*If your study involves multiple day surveys, then make sure to calculate the drift correction for each individual day. The drift equation for day 1 in the Example Spreadsheet is:*

**Day 1 (1/21/2006):**

$$X3 = ((W3 - W12) / E12) * E3$$

**Day 2 (1/22/2006):**

$$X13 = ((W13 - W22) / E22) * E3$$

**Day 3 (1/23/2006):**

$$X23 = ((W23 - W34) / E34) * E3$$

**Column Y: Drift & Tide Corrected (mgal)**

This column is the sum of the **Tide Corrected** column and the **Drift** column.

$$Y3 = W3 + X3$$

**Column Z: DC Shift**

In the Example Spreadsheet, the hypothetical absolute base station reading was measured during the first day of surveying (Row 11). To apply the DC shift, subtract the Tide and Drift Corrected (Column Y) base station readings for day 2 and day 3 (Y13 or Y22 for day 2, and Y23 or Y34 for day 3) from either base station reading for day 1 (Y3 or Y12). *The DC shift value for each day is a constant, so don't drag the equation down the column.*

DC Shift for Cell Z13 =Y12-Y13 = -1.539, which is the value used for all station readings for day 2 (1-22-2006)

**Column AA: Latitude Correction (mgal)**

This correction accounts for the increase in gravity with increasing latitude.

$$AA3 = (0.8108 * \text{SIN}(\text{RADIANS}(2 * L3)) * Q3)$$

**Column AB: Theoretical Gravity (mgals)**

The Somigliana closed-form formula (Hildenbrand, 2002) is used to calculate the theoretical gravity for each gravity station based on the GRS80 reference ellipsoid.

$$AB3 = 100000 * 9.7803267714 * ((1 + 0.00193185138639 * (\text{SIN}(L3 * (\text{PI}() / 180)))^2) / (\text{SQRT}(1 - 0.00669437999013 * (\text{SIN}(L3 * (\text{PI}() / 180)))^2)))$$

**Column AC: Height Correction (mgals)**

This column corrects for the height relative to the GRS80 ellipsoid.

$$AC3 = -0.308769097 * N3 + 0.000439773125 * N3 * ((\text{SIN}(L3 * (\text{PI}() / 180)))^2) +$$

$$0.0000000721251838*N3^2$$

**Column AD: *Atm Correction (mgal)***

This correction accounts for the mass of the atmosphere above the reference ellipsoid.

$$AD3 = 0.874 - 0.000099*N3 + 0.00000000356*N3^2$$

**Column AE: *Bouguer Spherical Cap (mgal)***

The Bouguer Spherical Cap is the new standard method that accounts for the average mass and curvature of the Earth with respect to the ellipsoid. This calculation uses the Bullard B Table to interpolate the correction between two sets of heights (m) above the ellipsoid. The default density of the Bouguer spherical cap is 2.67 g/cc (LaFehr 1991).

$$AE3 = (N3 - VLOOKUP(N3, 'Bullard B Table'!$A$4:$B$67, 1)) * ((VLOOKUP(N3 + 100, 'Bullard B Table'!$A$4:$B$67, 2) - VLOOKUP(N3, 'Bullard B Table'!$A$4:$B$67, 2)) / 100) + VLOOKUP(N3, 'Bullard B Table'!$A$4:$B$67, 2) + 2 * (PI()) * (0.00000000006673) * N3 * 2670 * 100000$$

**Column AF: *Terrain Correction (mgal)***

Terrain corrections need to be calculated using another software program. *Only enter the terrain correction value, not the sum of the observed gravity and terrain correction.*

**Column AG: *Observed Gravity (mgal)***

This column references the drift and tide corrected value in *Column X* to the absolute gravity base station and applies the DC shift and latitude correction. To complete this calculation, enter the base station information in the Absolute Base worksheet.

Absolute Base worksheet:

B3 is the latitude of the absolute base station in decimal degrees (DD).

B6 is the adopted absolute gravity value in mgals.

B15 is the reading of the gravity meter after it has been corrected for tide and drift. This value should be entered manually after calculating the value in *Column Y* of the Gravity worksheet.

$$AG3 = Y3 - 'Absolute Base'!B15 + 'Absolute Base'!B6 + Z3 + AA3$$

**Column AG: Complete Bouguer Anomaly (mgal)**

The complete Bouguer anomaly is the difference in observed gravity from the corrected theoretical gravity.

$$AG3 = AG3 - (AB3 + AC3 - AD3 + AE3 - AF3)$$

**REFERENCES CITED**

Cogbill, A.H., 1990, Gravity terrain corrections calculated using digital elevation models: *Geophysics*, v. 55, no. 1, p. 102-106.

Hildenbrand, T.G., Briesacher, A., Flanagan, G., Hinze, W.J., Hittelman, A.M., Keller, G.R., Kucks, R.P., Plouff, D., Roest, W., Seeley, J., Smith, D.A., and Webring, M., 2002, Rationale and Operational Plan to Upgrade the U.S. Gravity Database: U.S. Geological Survey Open-File Report 02-463, 12 p.

Hinze, W., Aiken, C., Brozena, J., Coakley, B., Dater, D., Flanagan, G., Forsberg, R., Hildenbrand, T., Keller, G.R., Kellogg, J., Kucks, R., Li, X., Mainville, A., Morin, R., Pilkington, M., Plouff, D., Ravat, D., Roman, D., Urrutia-Fucugauchi, J., Véronneau, M., Webring, M., and Winester, D., 2003, New standards for reducing gravity observations: The Revised North American Gravity Database <http://paces.geo.utep.edu/research/gravmag/PDF/Final%20NAGDB%20Report%20091403.pdf> Accessed 2006 March 6.

LaFehr, T.R., 1991, An exact solution for the gravity curvature (Bullard B) correction: *Geophysics*, v. 56, no. 8, p. 1179-1184.

National Geodetic Survey (NGS), 2006, [http://www.ngs.noaa.gov/PC\\_PROD/GEOID03/](http://www.ngs.noaa.gov/PC_PROD/GEOID03/) Accessed 2006 March 8.

Pan-American Center for Earth and Environmental Studies (PACES), 2006, <http://paces.geo.utep.edu/research/gravmag/gravmag.shtml> Accessed 2006 March 6.

### Appendix C. Kamiak Gap Gravity Data

Station	Latitude	Longitude	Ellipsoid Elevation (m)	Complete Bouguer Anomaly (mGal)	Residuals (mGal)
KMK001	46.85866	-117.08040	773.188	-113.86	-4.58
KMK002	46.85868	-117.08434	768.623	-114	-4.78
KMK003	46.85866	-117.08828	783.867	-115.36	-6.21
KMK004	46.85862	-117.09223	762.067	-114.61	-5.53
KMK005	46.85848	-117.09615	762.098	-115.06	-6.06
KMK006	46.85849	-117.10009	753.697	-114.82	-5.89
KMK007	46.85861	-117.10402	748.341	-114.62	-5.75
KMK008	46.85868	-117.10795	745.108	-114.24	-5.44
KMK009	46.85872	-117.11189	742.760	-113.85	-5.12
KMK010	46.85869	-117.11583	741.678	-113.1	-4.44
KMK011	46.85875	-117.11977	750.760	-113.33	-4.73
KMK012	46.85869	-117.12370	736.770	-111.79	-3.26
KMK013	46.85861	-117.12764	733.730	-111.32	-2.87
KMK014	46.85878	-117.13157	733.029	-111.03	-2.64
KMK015	46.86479	-117.07562	824.661	-112.08	-2.48
KMK016	46.86509	-117.07952	775.663	-113.16	-3.62
KMK017	46.86574	-117.08334	770.799	-114.9	-5.40
KMK018	46.86579	-117.08728	756.784	-113.69	-4.26
KMK019	46.86575	-117.09122	750.580	-113.67	-4.31
KMK020	46.86593	-117.09514	755.644	-113	-3.70
KMK021	46.86597	-117.09908	779.511	-113.99	-4.76
KMK022	46.86598	-117.10302	776.964	-114.64	-5.48
KMK023	46.86594	-117.10694	767.841	-114.7	-5.61
KMK024	46.86597	-117.11089	758.836	-114.1	-5.08
KMK025	46.86596	-117.11482	761.129	-113.08	-4.13
KMK026	46.86600	-117.11876	767.655	-113.34	-4.46
KMK027	46.86599	-117.12270	761.911	-112.57	-3.76
KMK028	46.86597	-117.12664	739.817	-110.62	-1.87
KMK029	46.86599	-117.13058	774.900	-109.51	-0.83
KMK030	46.86592	-117.13451	804.734	-108.66	-0.05
KMK031	46.87546	-117.05700	819.737	-112.38	-2.06
KMK032	46.87340	-117.05796	797.474	-113.02	-2.79
KMK033	46.87322	-117.06188	764.427	-112.07	-1.92
KMK034	46.87329	-117.06583	763.098	-113.1	-3.01
KMK035	46.87330	-117.06977	761.229	-112.15	-2.13
KMK036	46.87354	-117.07369	759.222	-111.7	-1.74
KMK037	46.87321	-117.07760	759.913	-111.31	-1.43
KMK038	46.87324	-117.08153	775.023	-112.31	-2.50
KMK039	46.87325	-117.08547	767.842	-112.49	-2.75
KMK040	46.87315	-117.08940	770.483	-113.22	-3.55
KMK041	46.87328	-117.09334	764.414	-113.46	-3.86
KMK042	46.87325	-117.09727	778.010	-114.89	-5.36
KMK043	46.87322	-117.10120	783.684	-114.84	-5.38
KMK044	46.87324	-117.10513	774.233	-114.62	-5.23
KMK045	46.87329	-117.10907	756.981	-113.14	-3.81
KMK046	46.87332	-117.11300	771.203	-113.65	-4.39

KMK047	46.87339	-117.11694	762.215	-112.81	-3.62
KMK048	46.87369	-117.12085	755.504	-112.14	-3.01
KMK049	46.87428	-117.12470	743.861	-111.78	-2.69
KMK050	46.87324	-117.09168	758.964	-112.82	-3.19
KMK051	46.86814	-117.09150	752.777	-113.35	-3.91
KMK052	46.85869	-117.10579	748.430	-113.93	-5.09
KMK053	46.85880	-117.10619	746.606	-113.88	-5.04
KMK054	46.85983	-117.10403	747.348	-114.14	-5.23
KMK055	46.86090	-117.10191	747.887	-113.42	-4.43
KMK056	46.86197	-117.09980	748.551	-113.16	-4.09
KMK057	46.86297	-117.09763	750.212	-112.98	-3.84
KMK058	46.86409	-117.09558	751.832	-113.2	-3.98
KMK059	46.86553	-117.09397	750.896	-113.16	-3.86
KMK060	46.86795	-117.09226	753.980	-113.04	-3.62
KMK061	46.87039	-117.09076	755.597	-112.7	-3.16
KMK062	46.87324	-117.09167	758.892	-112.6	-2.97
KMK063	46.86619	-117.07488	816.799	-112.81	-3.15
KMK064	46.86608	-117.07699	785.193	-112.56	-2.94
KMK065	46.86599	-117.07777	788.849	-113	-3.40
KMK066	46.86598	-117.07976	766.322	-112.77	-3.20
KMK067	46.86594	-117.08240	775.557	-115.01	-5.49
KMK068	46.86605	-117.08680	760.146	-113.73	-4.28
KMK069	46.86599	-117.09270	750.972	-113.25	-3.91
KMK070	46.86595	-117.09471	754.545	-113.1	-3.80
KMK071	46.86593	-117.09783	777.495	-114.04	-4.79
KMK072	46.86596	-117.10079	769.912	-113.22	-4.02
KMK073	46.86595	-117.10251	784.491	-114.89	-5.72
KMK074	46.86597	-117.10483	761.378	-113.76	-4.63
KMK075	46.86597	-117.10857	775.573	-114.88	-5.82
KMK076	46.86596	-117.11190	751.579	-113.06	-4.06
KMK077	46.86588	-117.11305	750.185	-112.82	-3.84
KMK078	46.86598	-117.11505	762.743	-113.15	-4.20
KMK079	46.86600	-117.11769	775.377	-113.79	-4.89
KMK080	46.86601	-117.11941	765.032	-113.18	-4.31
KMK081	46.86589	-117.12070	769.678	-113.52	-4.67
KMK082	46.86589	-117.12245	763.155	-112.7	-3.88
KMK083	46.86589	-117.12586	742.387	-111.04	-2.28
KMK084	46.87349	-117.11708	761.784	-112.72	-3.53
KMK085	46.85855	-117.11724	745.855	-113.06	-4.43
KMK086	46.86593	-117.13560	814.266	-108.96	-0.37
KMK087	46.86604	-117.13839	814.231	-108.82	-0.28
KMK088	46.85823	-117.07486	788.711	-113.45	-4.08
KMK089	46.85868	-117.07720	779.879	-113.74	-4.40
KMK090	46.85890	-117.08029	771.758	-113.64	-4.34
KMK091	46.85890	-117.08195	779.200	-113.98	-4.71
KMK092	46.85875	-117.08379	769.630	-113.65	-4.42
KMK093	46.85870	-117.08743	787.640	-114.99	-5.83
KMK094	46.85871	-117.09076	763.912	-114.21	-5.11
KMK095	46.85870	-117.09374	778.744	-115.33	-6.28
KMK096	46.85864	-117.09589	764.727	-114.81	-5.80

KMK097	46.85865	-117.09770	757.309	-114.57	-5.59
KMK098	46.85882	-117.10143	748.925	-114.04	-5.12
KMK099	46.85875	-117.10379	748.672	-114.18	-5.30
KMK100	46.85868	-117.10645	746.751	-113.82	-4.99
KMK101	46.85863	-117.10886	745.462	-113.91	-5.13
KMK102	46.85866	-117.11142	743.391	-113.51	-4.77
KMK103	46.85876	-117.11446	741.549	-113.31	-4.62
KMK104	46.85881	-117.11664	746.731	-112.98	-4.33
KMK105	46.85878	-117.12170	739.620	-111.98	-3.42
KMK106	46.85867	-117.12583	734.999	-111.07	-2.58
KMK107	46.85839	-117.12809	733.736	-111.19	-2.75
KMK108	46.85877	-117.10563	752.704	-113.44	-4.59
KMK109	46.86596	-117.09330	753.413	-113.14	-3.81
KMK110	46.87326	-117.09171	759.164	-112.66	-3.03
KMK111	46.87653	-117.08961	763.139	-112.6	-2.81
KMK112	46.88220	-117.08908	766.747	-114.3	-4.29
KMK113	46.88460	-117.08773	762.550	-114.99	-4.87
KMK114	46.88736	-117.08426	757.518	-115.32	-5.04
KMK115	46.89009	-117.08227	753.135	-115.59	-5.17
KMK116	46.89282	-117.08078	750.144	-116.02	-5.47
KMK117	46.89552	-117.07942	746.324	-115.99	-5.32
KMK118	46.89822	-117.07805	743.307	-115.8	-5.00
KMK119	46.90125	-117.07693	738.296	-116.44	-5.51
KMK120	46.90400	-117.07740	733.407	-116.68	-5.66
KMK121	46.90706	-117.07862	727.858	-117.1	-5.98
KMK122	46.90586	-117.08296	746.322	-116.8	-5.81
KMK123	46.85652	-117.11005	750.172	-114.33	-5.65
KMK124	46.85519	-117.11403	751.305	-114.33	-5.76
KMK125	46.85247	-117.11910	755.665	-113.71	-5.33
KMK126	46.84941	-117.12110	752.856	-113.75	-5.52
KMK127	46.84670	-117.12205	749.787	-113.04	-4.93
KMK128	46.84400	-117.12373	746.569	-111.75	-3.77
KMK129	46.84134	-117.12346	743.872	-111.99	-4.10
KMK130	46.83886	-117.11965	739.366	-112.55	-4.69
KMK131	46.90950	-117.08044	720.631	-115.8	-4.63
KMK132	46.93010	-117.07493	747.451	-119.27	-7.23
KMK133	46.91264	-117.07998	751.101	-117.3	-6.00





The Department of Ecology does NOT Warranty the Data and/or the Information on this Well Report.

# WATER WELL REPORT

Original & 1st copy - Ecology, 2nd copy - owner, 3rd copy - driller

Construction/Decommission ("x" in circle) **107515**  
 Construction  
 Decommission ORIGINAL CONSTRUCTION Notice of Intent Number \_\_\_\_\_

CURRENT Notice of Intent No. W065633

Unique Ecology Well ID Tag No. AAW758

Water Right Permit No. \_\_\_\_\_

Property Owner Name Walter Lundford

Well Street Address \_\_\_\_\_  
City Palouse County: Whitman

Location NE 1/4 SE 1/4 Sec 19 Twn 16 R46 EWM circle or one WWM

Lat/Long: Lat Deg \_\_\_\_\_ Lat Min/Sec \_\_\_\_\_  
(s.t.r still REQUIRED) Long Deg \_\_\_\_\_ Long Min/Sec \_\_\_\_\_

Tax Parcel No. \_\_\_\_\_

PROPOSED USE:  Domestic  Industrial  Municipal  
 DeWater  Irrigation  Test Well  Other

TYPE OF WORK: Owner's number of well (if more than one) \_\_\_\_\_  
 New Well  Reconditioned Method:  Dug  Bored  Driven  
 Deepened  Cable  Rotary  Jetted

DIMENSIONS: Diameter of well 6" inches, drilled 450 ft.  
Depth of completed well 450 ft.

CONSTRUCTION DETAILS  
Casing  Welded  Diam. from +2 ft. to 275 ft.  
Installed:  Liner installed 4 1/2" Diam. from -200 ft. to 450 ft.  
 Threaded Diam. from \_\_\_\_\_ ft. to \_\_\_\_\_ ft.

Perforations:  Yes  No  
Type of perforator used ann cut  
SIZE of perfs. 3 in. by 1/8 in. and no. of perfs. 200 from 391 ft. to 450 ft.

Screens:  Yes  No  K-Pac Location \_\_\_\_\_  
Manufacturer's Name \_\_\_\_\_ Model No. \_\_\_\_\_  
Type \_\_\_\_\_ Slot Size \_\_\_\_\_ from \_\_\_\_\_ ft. to \_\_\_\_\_ ft.  
Diam. \_\_\_\_\_ Slot Size \_\_\_\_\_ from \_\_\_\_\_ ft. to \_\_\_\_\_ ft.

Gravel/Filter packed:  Yes  No  Size of gravel/sand \_\_\_\_\_ ft. to \_\_\_\_\_ ft.  
Materials placed from \_\_\_\_\_ ft. to \_\_\_\_\_ ft.

Surface Seal:  Yes  No To what depth? 70 ft.  
Materials used in seal Benfrate  
Did any strata contain unusable water?  Yes  No  
Type of water? \_\_\_\_\_ Depth of strata \_\_\_\_\_  
Method of sealing strata off \_\_\_\_\_

PUMP: Manufacturer's Name \_\_\_\_\_  
Type: \_\_\_\_\_ H.P. \_\_\_\_\_

WATER LEVELS: Land-surface elevation above mean sea level \_\_\_\_\_ ft.  
Static level 120 ft. below top of well Date \_\_\_\_\_  
Artesian pressure \_\_\_\_\_ lbs. per square inch Date \_\_\_\_\_  
Artesian water is controlled by \_\_\_\_\_ (cap, valve, etc.)

WELL TESTS: Drawdown is amount water level is lowered below static level.  
Was a pump test made?  Yes  No If yes, by whom? \_\_\_\_\_  
Yield: \_\_\_\_\_ gal./min. with \_\_\_\_\_ ft. drawdown after \_\_\_\_\_ hrs.  
Yield: \_\_\_\_\_ gal./min. with \_\_\_\_\_ ft. drawdown after \_\_\_\_\_ hrs.  
Yield: \_\_\_\_\_ gal./min. with \_\_\_\_\_ ft. drawdown after \_\_\_\_\_ hrs.

Recovery data (time taken as zero when pump turned off) (water level measured from well top to water level)  
Time Water Level Time Water Level Time Water Level  
\_\_\_\_\_  
\_\_\_\_\_  
\_\_\_\_\_

Date of test \_\_\_\_\_  
Bailer test \_\_\_\_\_ gal./min. with \_\_\_\_\_ ft. drawdown after \_\_\_\_\_ hrs.  
Airstest 3 gal./min. with stem set at 450 ft. for 1 1/2 hrs.  
Artesian flow \_\_\_\_\_ g.p.m. Date \_\_\_\_\_  
Temperature of water \_\_\_\_\_ Was a chemical analysis made?  Yes  No

CONSTRUCTION OR DECOMMISSION PROCEDURE  
Formation: Describe by color, character, size of material and structure, and the kind and nature of the material in each stratum penetrated, with at least one entry for each change of information. Indicate all water encountered.  
(USE ADDITIONAL SHEETS IF NECESSARY.)

MATERIAL	FROM	TO
dirt	0	2
clay	2	27
soft clayey silt	27	280
gravel with diff colors, very soft		
fine brown	280	298
soft med soft	298	380
blue gravel	380	380
brown gravel	380	450

**RECEIVED**

DEC 28 2001

DEPARTMENT OF ECOLOGY  
WELL DRILLING UNIT

JAN 4 2002

DEPARTMENT OF ECOLOGY  
REGIONAL OFFICE

Start Date Oct 20, 01 Completed Date Oct 25, 01

WELL CONSTRUCTION CERTIFICATION: I constructed and/or accept responsibility for construction of this well, and its compliance with all Washington well construction standards. Materials used and the information reported above are true to my best knowledge and belief.

Driller  Engineer  Trainee Name (Print) Wm. Sheldoff  
Driller/Engineer/Trainee Signature Wm. Sheldoff  
Driller or Trainee License No. 1740

Drilling Company Whitcomb  
Address R1 Red 20  
City, State, Zip Fenn Id 83531  
Contractor's Registration No. \_\_\_\_\_ Date Dec 21, 01

If trainee, licensed driller's Signature and License no. \_\_\_\_\_

The Department of Ecology does NOT Warranty the Data and/or the Information on this Well Report.

File Original with Department of Ecology  
 Second Copy - Owner's Copy  
 Third Copy - Driller's Copy

74959

# WATER WELL REPORT

STATE OF WASHINGTON

Notice of Intent W121477

UNIQUE WELL ID # ACW-666

Water Right Permit No G3-24434P

(1) OWNER: Name City of Palouse %Kimball Eng. Address 114 Thain Rd, Lewiston Id 83501

(2) LOCATION OF WELL: County Whitman NE 1/4 SE 1/4 Sec. 01 T 16 N R 46E WM

(2a) STREET ADDRESS OF WELL (or nearest address) \_\_\_\_\_

TAX PARCEL NO \_\_\_\_\_

(3) PROPOSED USE:  Domestic  Industrial  Municipal  
 Irrigation  Test Well  Other  
 DeWater

(4) TYPE OF WORK: Owner's number of well (if more than one) \_\_\_\_\_  
 New Well Method  Bored  
 Deepened  Dug  Driven  
 Reconditioned  Cable  Jetted  
 Decommission  Rotary

(5) DIMENSIONS: Diameter of well 16" and 12" inches  
 Drilled 460 feet Depth of completed well 432.5 ft

(6) CONSTRUCTION DETAILS  
 Casing Installed  
 Welded 12" Diam from +3 ft to 400 ft  
 Liner installed Diam from \_\_\_\_\_ ft to \_\_\_\_\_ ft  
 Threaded Diam from \_\_\_\_\_ ft to \_\_\_\_\_ ft

Perforations:  Yes  No  
 Type of perforator used \_\_\_\_\_  
 SIZE of perforations \_\_\_\_\_ in by \_\_\_\_\_ in  
 \_\_\_\_\_ perforations from \_\_\_\_\_ ft to \_\_\_\_\_ ft

Screens.  Yes  No  K-Pac Location \_\_\_\_\_  
 Manufacturer's Name \_\_\_\_\_  
 Type Stainless Steel Model No \_\_\_\_\_  
 Diam 10" Slot Size 150 from -397.9 ft to 432.5 ft  
 Diam \_\_\_\_\_ Slot Size \_\_\_\_\_ from \_\_\_\_\_ ft to \_\_\_\_\_ ft

Gravel/Filter packed:  Yes  No  Size of gravel/sand 3/8 minis  
 Material placed from 432.5 ft to 444 ft

Surface seal:  Yes  No To what depth? 400' ft  
 Material used in seal Cement  
 Did any strata contain usable water?  Yes  No  
 Type of water? Surface Depth of strata 200  
 Method of sealing strata off Cased off and cemented

(7) PUMP: Manufacturer's Name \_\_\_\_\_  
 Type \_\_\_\_\_ H P \_\_\_\_\_

(8) WATER LEVELS: Land-surface elevation above mean sea level \_\_\_\_\_ ft  
 Static level 250 ft below top of well Date \_\_\_\_\_  
 Artesian pressure \_\_\_\_\_ lbs per square inch Date \_\_\_\_\_  
 Artesian water is controlled by \_\_\_\_\_  
 (Cap, valve, etc.)

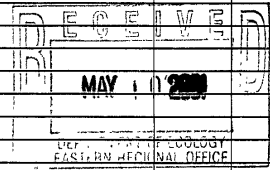
(9) WELL TESTS: Drawdown is amount water level is lowered below static level  
 Was a pump test made?  Yes  No If yes, by whom? H2O Well Svc  
 Yield 800+ gal/min with \_\_\_\_\_ ft drawdown after \_\_\_\_\_ hrs  
 Yield \_\_\_\_\_ gal/min with \_\_\_\_\_ ft drawdown after \_\_\_\_\_ hrs  
 Yield \_\_\_\_\_ gal/min with \_\_\_\_\_ ft drawdown after \_\_\_\_\_ hrs  
 Recovery data (time taken as zero when pump turned off) (water level measured from well top to water level)  

Time	Water Level	Time	Water Level	Time	Water Level
_____	_____	_____	_____	_____	_____
_____	_____	_____	_____	_____	_____

 Date of test \_\_\_\_\_  
 Bailor test \_\_\_\_\_ gal/min with \_\_\_\_\_ ft drawdown after \_\_\_\_\_ hrs  
 Airtest 800+ gal/min with \_\_\_\_\_ ft drawdown after \_\_\_\_\_ hrs  
 Artesian flow \_\_\_\_\_ g p m Date \_\_\_\_\_  
 Temperature of water \_\_\_\_\_ Was a chemical analysis made?  Yes  No

(10) WELL LOG or DECOMMISSIONING PROCEDURE DESCRIPTION  
 Formation Describe by color, character, size of material and structure, and the kind and nature of the material in each stratum penetrated, with at least one entry for each change of information Indicate all water encountered

MATERIAL	FROM	TO
Topsoil	0	3
Basalt Fractured	3	188
Sand Fine W/Water	188	218
Clay Blue Gray W/Sand	218	312
Clay Brown W/Basalt Chips	312	319
Clay Brown W/Sand	319	330
Basalt W/Clay Seams	330	358
Clay W/Basalt Chips	358	368
Clay Brown W/Sand	368	395
Basalt Hard	395	402
Basalt Fractured W/Water	402	420
Basalt Hard	420	423
Basalt Fractured W/Water	423	435
Basalt Hard	435	447
Basalt W/Green Hard Clay	447	449
Basalt Broken	449	460



Work Started 12/03/99 Completed 01/13/00

**WELL CONSTRUCTION CERTIFICATION:**

I constructed and/or accept responsibility for construction of this well, and its compliance with all Washington well construction standards. Material used and the information reported above are true to my best knowledge and belief

Type or Print Name Louie Hanner License No 1472  
 (Licensed Driller/Engineer)

Trainee Name \_\_\_\_\_ License No \_\_\_\_\_  
 Drilling Company H2O WELL SVC 1-800-772-4901  
 (Signed) \_\_\_\_\_ License No 1472  
 (Licensed Driller/Engineer)

Address 582 W Hayden Ave Hayden Lake Id 838

Contractor's Registration No H2OWESI101DW Date 01/19/00

(USE ADDITIONAL SHEETS IF NECESSARY)

Ecology is an Equal Opportunity and Affirmative Action employer For special accommodation needs, contact the Water Resources Program at (360) 407-6600 The TDD number is (360) 407-6006



### Appendix E. Structural contour map of the basement in the Kamiak Gap.

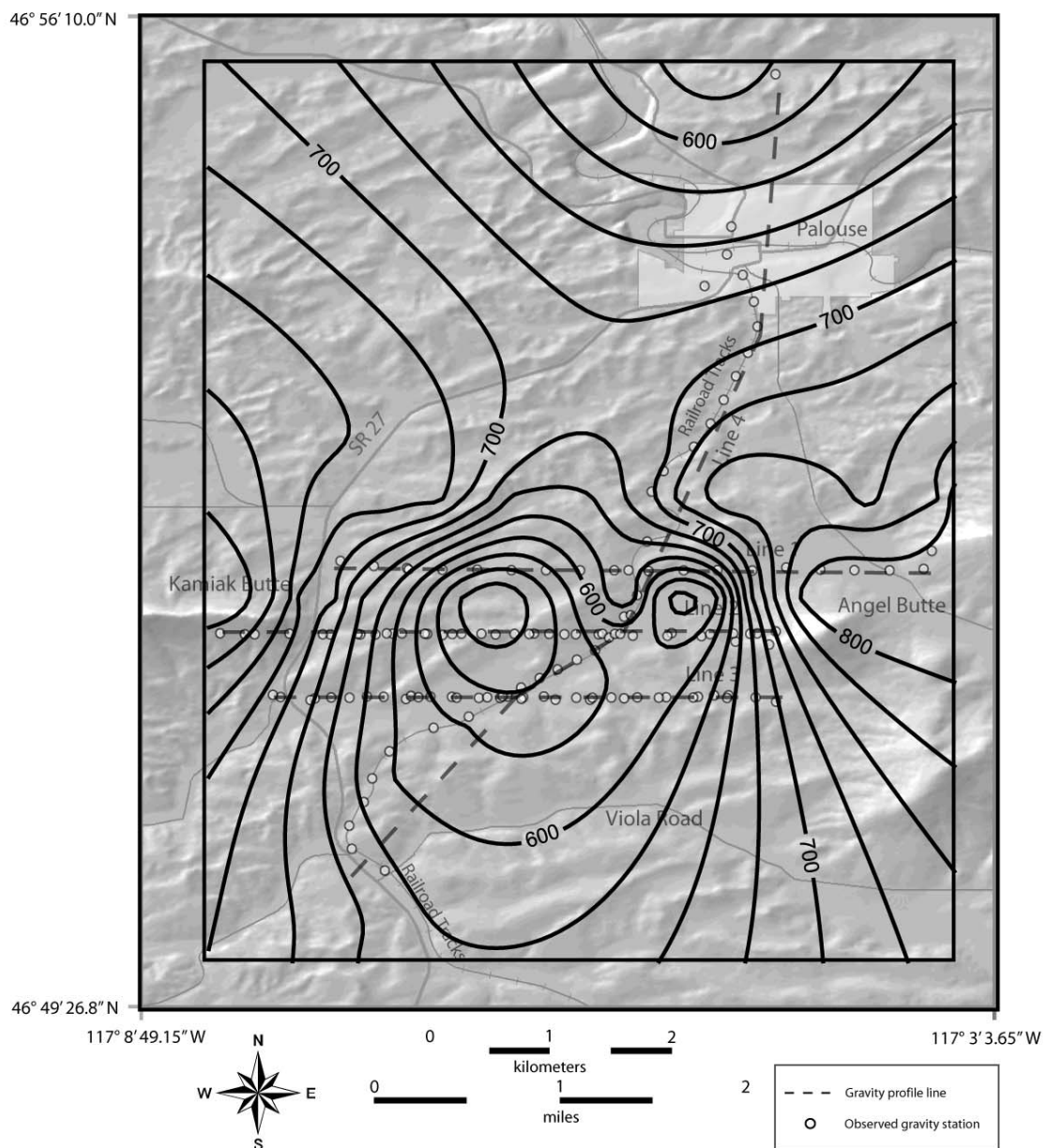


**Figure A. Structural contour map of the basement in the Kamiak Gap. Elevation of the contour lines are with respect to the WGS84 ellipsoid and are in meters. The contour interval is 25 meters.**

Appendix F. Contour map of the regional Bouguer anomalies.

